Exploring the roles of numerical simulations and machine learning in multiscale paving materials analysis

Applications, challenges, best practices

Khadijeh, Mahmoud; Kasbergen, Cor; Erkens, Sandra; Varveri, Aikaterini

DOI
10.1016/j.cma.2024.117462

Publication date
2024

Document Version
Final published version

Published in
Computer Methods in Applied Mechanics and Engineering

Computer Methods in Applied Mechanics and Engineering 433 (2025) 117462

Contents lists available at ScienceDirect

Comput. Methods Appl. Mech. Engrg.

journal homepage: www.elsevier.com/locate/cma

Exploring the roles of numerical simulations and machine learning in multiscale paving materials analysis: Applications, challenges, best practices

Mahmoud Khadijeh *, Cor Kasbergen, Sandra Erkens, Aikaterini Varveri

Department of Engineering Structures, Delft University of Technology, Stevinweg 1, Delft, 2628 CN, Netherlands

GRAPHICAL ABSTRACT

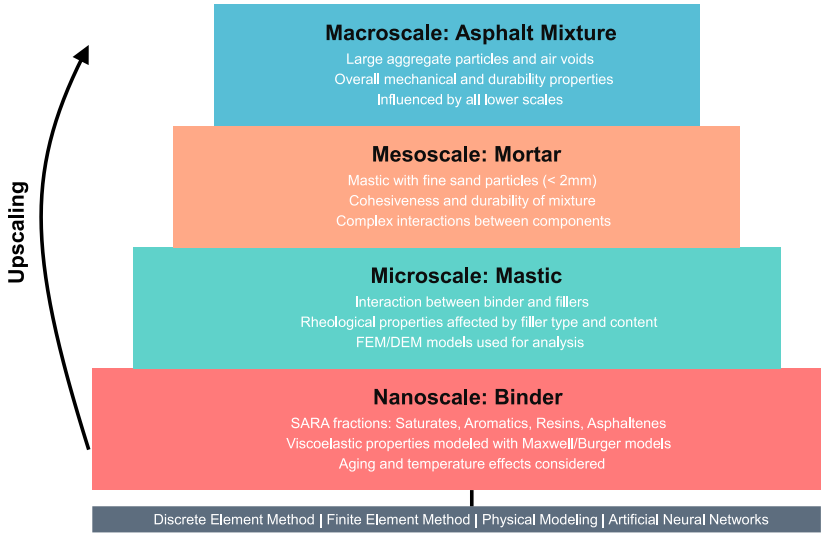

ARTICLE INFO

Keywords:
Multiscale modeling
Paving materials
Numerical simulation
Machine learning
Finite element method
Discrete element method

ABSTRACT

The complex structure of bituminous mixtures ranging from nanoscale binder components to macroscale pavement performance requires a comprehensive approach to material characterization and performance prediction. This paper provides a critical analysis of advanced techniques in paving materials modeling. It focuses on four main approaches: finite element method (FEM), discrete element method (DEM), phase field method (PFM), and artificial neural networks (ANNs). The review highlights how these computational methods enable more accurate predictions of material behavior, from asphalt binder rheology to mixture

* Corresponding author.
E-mail address: m.khadijeh@tudelft.nl (M. Khadijeh).

https://doi.org/10.1016/j.cma.2024.117462
Received 3 May 2024; Received in revised form 19 September 2024; Accepted 10 October 2024
Available online 28 October 2024

Physics informed neural networks

performance, while reducing reliance on extensive empirical testing. Key advances, such as the smooth integration of information across multiple scales and the emergence of physics-informed neural networks (PINNs), are discussed as promising avenues for enhancing model accuracy and computational efficiency. This review not only provides a comprehensive overview of current methodologies but also outlines future research directions aimed at developing more sustainable, cost-effective, and durable paving solutions through advanced multiscale modeling techniques.

Contents

1. Introduction

Multiscale modeling is a sophisticated approach to modeling that involves analyzing the behavior of entities across different scales to understand how they operate and interact with each other [1,2]. This methodology is useful for addressing complex challenges that exhibit significant characteristics across multiple dimensions of time and/or space [3,4]. In civil engineering, multiscale modeling is a crucial tool for analyzing the behavior of complex materials, including concrete, rocks, and asphalt mixtures [3–5]. Through the integration of various scales of material and structural interactions, multiscale modeling improves material design and construction practices [6].

In the field of pavement engineering, multiscale modeling is essential for designing and analyzing asphalt mixtures. Asphalt mixtures are the most commonly used material for road construction in the pavement sector. It is influenced by several factors, including the natural variability of the materials used, reflected by their strength, dimensions, and chemical composition. The properties of the aggregate and fillers, as well as the category of binders employed, also contribute to the overall performance. Environmental influences such as aging and weathering are additional determinants. Furthermore, the actual performance in the field, coupled with the methodologies employed for testing and characterization, are critical considerations. Understanding and optimizing these factors allows for the design and construction of high-quality, long-lasting pavements that can withstand various conditions while minimizing environmental impact, reducing costs, and enhancing safety [7–10].

In light of the intricate and interconnected nature of the factors influencing asphalt mixture performance and pavement construction, it is crucial to employ a comprehensive and sophisticated approach to modeling and simulation. However, the challenges associated with modeling and simulation in pavement engineering are significant, including the need to account for the complex interplay between material properties, structural behavior, and environmental factors. In addition to the large number of variables involved, the high dimensionality of the problem space makes it difficult to develop accurate and reliable models. Despite these challenges, the potential benefits of advanced modeling and simulation in pavement engineering are substantial. Numerical methods such as the finite element method (FEM), discrete element method (DEM), phase field method (PFM), and micromechanical analytical models, along with machine learning (ML) algorithms, emerge as promising approaches [11]. The core objective of this paper is to provide a critical analysis of how numerical methods and machine learning algorithms are applied in multiscale modeling of paving materials. The study examines in depth the constraints and challenges encountered when modeling and simulating these materials. Additionally, the paper explores potential future directions in this field, suggesting areas where research could be focused to overcome current limitations and advance the understanding and modeling capabilities of paving materials.

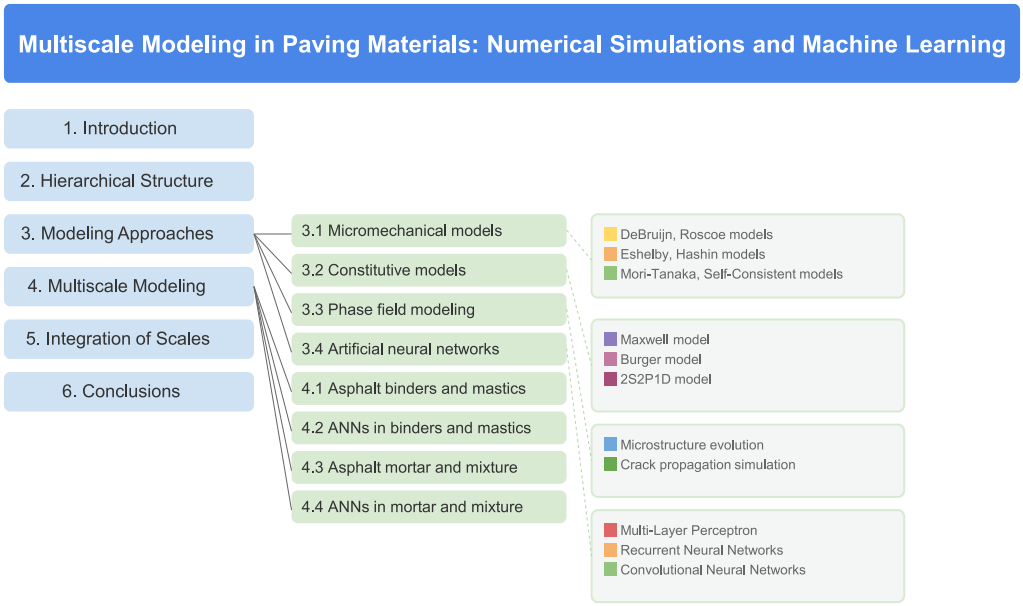

Fig. 1. Review paper's framework — an overview of methodologies and predictive strategies for paving materials.

The first half of the study focuses primarily on clarifying the hierarchical structure of bituminous mixture, from nanoscale to macroscale level. This involves addressing the complexities inherent in modeling the distinct behaviors exhibited by individual components across varying scales. Section 3 presents a thorough examination of the multiscale modeling approaches, including micromechanical models, constitutive models, PFM, and artificial neural networks (ANNs). Section 4 explores the practical applications of these modeling techniques at different scales, from asphalt binders and mastics to mortars and mixtures. Finally, Section 5 addresses the integration of all scales, current limitations, and future research directions in multiscale modeling of bituminous mixtures. Fig. 1 provides a visual representation of the paper's organization, serving as a useful guide for navigating the content of the manuscript.

2. Hierarchical structure and influencing factors of bituminous mixtures: a comprehensive study overview

The behavior of asphalt mixtures is influenced by a variety of factors that span multiple scales, from the nanoscale to the macroscale (Fig. 2). Asphalt binder, which is characterized by polarity into saturates, aromatics, resins, and asphaltenes (often referred to as SARA fractions), demonstrates a complex composition at the nanoscale. While the exact distribution of these component fractions within the binder matrix remains a topic of ongoing debate, research has shown that they can be randomly dispersed. For instance, previous research has challenged the traditional understanding of asphalt binder's molecular structure [13]. Instead of the widely accepted belief that asphalt binder components form micellar structures, this research suggested that asphalt binder is a complex blend of intermingled molecules in a state of mutual solubility. This non-micellar model highlights the impact of molecular polarity on binder's properties, such as elasticity, at working temperatures, providing a more detailed insight into the behavior of asphalt binder at the nanoscale. Conversely, it has been suggested that asphalt binder forms a colloidal model, in which asphaltenes and resins create micelle chains surrounded by saturates and aromatics [11,14]. These contrasting theories underscore the complexity of binder's molecular structure and the impact of molecular polarity on its properties.

Given the complex molecular structure of asphalt binder and the significant role of SARA fractions, many steps have been taken to comprehend their impact on the behavior of asphalt binder and subsequently, the behavior of the upper scales. For instance, asphaltenes, which are the heavier and more polar constituents within the entire spectrum of asphalt molecules, have been found to be directly related to the appearance of the bee structure. The bee structure represents points in the material that are susceptible to the initiation of microcracks. These microcracks can expand under applied loads, emphasizing their role in the overall behavior of the bituminous material [13,15]. This structure is a critical concept as it helps in understanding how the material respond under certain conditions.

Asphalt binder, on the other hand, undergoes short-term and long-term aging, which significantly influences how the pavement behaves during its service life. Short-term aging occurs during the production, construction, and storage of asphalt binders. Long-term aging represents the thermal and oxidative aging of asphalt binder during the pavement service life and is mostly driven by environmental exposure and loads [16]. A significant study in this field developed an aging protocol to understand how oxidative aging affects the mechanical and chemical properties of asphalt pavements [10]. This research utilized both field-collected samples and laboratory aging simulations. The findings highlighted the spatial variability of aging within the pavement layers and emphasized that aging processes in real world conditions are more complex than those in controlled laboratory settings.

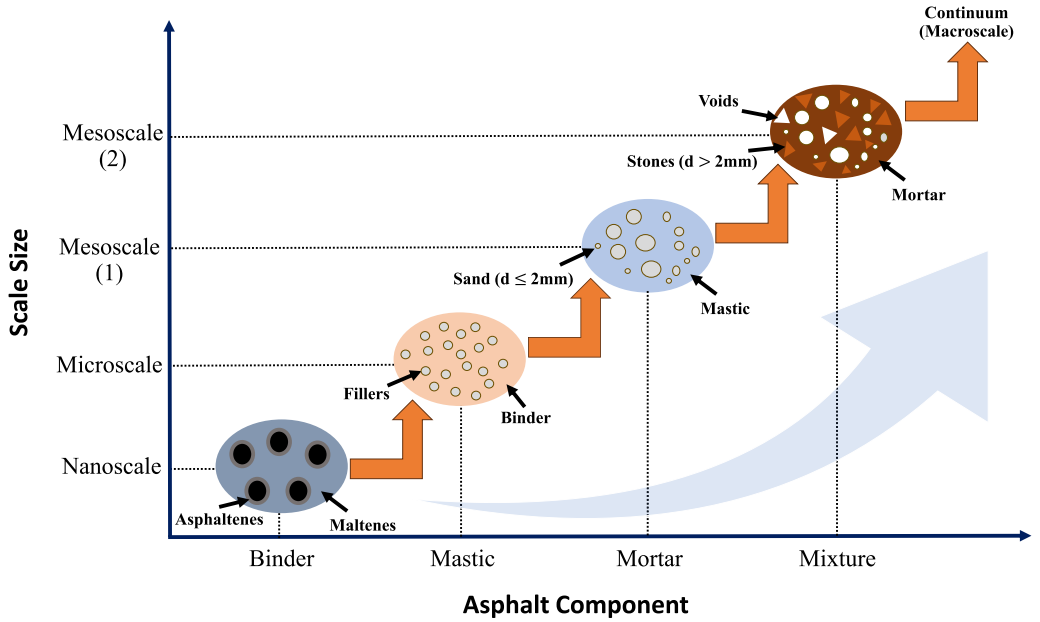

Fig. 2. Hierarchical structure, including the asphalt binder scale (bitumen), mastic-scale (bitumen + filler), mortar-scale (mastic + sand particles), and asphalt mixture scale, adapted from [12].

Moving from the nanoscale to larger structural elements, the "mastic" is recognized at the microscale. The mastic is composed of fillers distributed throughout an asphalt binder matrix at a specific volume percentage. At this scale, the selection of filler material and the rheological properties of asphalt binders are crucial in determining the bonding behavior between asphalt and aggregate in pavement structures. Numerous studies have explored this intricate relationship, shedding light on how different variables come into play. For instance, a recent study investigated how different filler materials, asphalt mastic properties, and water immersion conditions interact and influence the bonding behavior between asphalt mastics and aggregates in asphalt mixture [17]. Additionally, investigations into the effects of fillers on asphalt binder have revealed their favorable impact on mitigating age-hardening, linking this to oxygen transport and adsorption processes [18–20]. A comprehensive framework was developed to understand the interactions between various filler materials and asphalt binder in asphalt mastic, demonstrating how these interactions influence mastic's stiffness and shearing behavior [21]. Further research also examined the impact of active fillers on the rheological properties and fatigue resistance of Cold Bitumen Emulsion (CBE) mastics used in pavement construction [22]. This study emphasizes how the type of filler chosen and its chemical characteristics may impact how well CBE mixes operate, with some fillers enhancing the material's stiffness and fatigue resistance.

Shifting to the mesoscale level, which holds significant importance in bituminous research. The mesoscale level focuses on the complex interactions between the mortar and larger aggregate particles. This level can be further divided into two main components: the mortar and the mixture. The mortar is primarily made up of mastic and fine sand particles with diameters less than 2 mm. The mortar plays a crucial role in providing cohesiveness and durability to the asphalt mixture by acting as a glue that holds the larger aggregates together and fills the voids between them. The mixture component consists of aggregate particles of varying sizes and shapes, which form the structure of the asphalt mixture, as well as the voids created between them and the mortar. These voids have a significant impact on properties such as permeability, density, and thermal conductivity. The interplay between the mortar, aggregates, and voids is what gives asphalt mixtures their unique mechanical and functional characteristics [12].

Various studies have highlighted the importance of examining asphalt mixtures. For instance, innovative algorithms have been developed to identify and quantify the various elements within the asphalt mixtures to better understanding of their compositions and behaviors [23]. Research has also highlighted the influence of aggregate shapes on asphalt adhesion and the resulting mechanical properties, emphasizing the need to consider aggregate morphology during pavement design [24]. Additionally, new testing techniques have been proposed to understand the behavior of asphalt mixtures under complex stress conditions [25]. These studies underscore the importance of studying asphalt mixtures to enhance their performance and durability. Owing to the aforementioned impacts, it is essential to combine information from different scales to create a comprehensive multiscale framework that identify the key factors influencing the ultimate behavior of asphalt mixture.

Table 1
Predictive analytical models for determining effective properties of composite materials: G_c = modulus of the composite; G_m = modulus of the matrix; G_p = modulus of the particle inclusions; C_v = volume concentration of the particle inclusions; v_m = Poisson's ratio of the matrix.

Model	Equation	
DeBruijn	$\frac{G_c}{G_m} = 1 + 2.5C_v + 1.55C_v^2$	(1)
Roscoe	$\frac{G_c}{G_m} = (1 - C_v)^{-2.5}$	(2)
Eshelby	$\frac{G_c}{G_m} = 1 - \frac{15(1 - v_m)(1 - \frac{G_p}{G_m})}{7 - 5v_m + 2(4 - 5v_m)\frac{G_p}{G_m}} C_v$	(3)
Hashin	$\frac{G_c}{G_m} = 1 - \frac{15(1 - v_m)(1 - \frac{G_p}{G_m})C_v}{7 - 5v_m + 2(4 - 5v_m)[\frac{G_p}{G_m} - (\frac{G_p}{G_m} - 1)C_v]}$	(4)
Mori–Tanaka	$\frac{G_c}{G_m} = 1 + \frac{5C_v(G_p - G_m)}{5G_m + 2(1 - C_v)(G_p - G_m)}$	(5)
GSCM	$a(\frac{G_c}{G_m})^2 + b(\frac{G_c}{G_m}) + c = 0$	(6)

3. Multiscale modeling approaches for paving mixtures

3.1. Micromechanical models

Multiscale modeling involves studying complex systems by breaking them down into smaller, lower-dimensional components and understanding their behavior. This requires a detailed examination of the lower-dimensional components to identify the key factors that influence their behavior. One of the key approaches in multiscale modeling is the use of analytical micromechanical models, which offer a mathematical representation of the microstructure of materials. These models are built upon fundamental material properties such as Poisson's ratio, elastic modulus, and the volume fraction of different components within the material. They incorporate particle interactions through effective medium techniques, which allows for the prediction of large scale material behavior based on microscopic components. There are several such representations, including those by DeBruijn, Roscoe, as well as the Eshelby, Hashin, Mori–Tanaka, and Generalized Self-Consistent approaches. The DeBruijn model is a mathematical model used to predict the effective properties of a composite material. It examines the distribution of inclusions, such as particles or fibers, within a matrix [26]. The Roscoe model is a widely used model in geomechanics and soil mechanics to describe the behavior of granular materials, such as soils, by analyzing the arrangement of particles and their interactions. It is particularly useful for modeling soil deformation and strength. The Eshelby model is a mathematical framework for examining how stress and strain are distributed in materials with heterogeneities like inclusions or flaws [27]. This model allows researchers to better understand how the presence of these inclusions affects the overall mechanical behavior of the material. Building upon the Eshelby model, the Hashin model provides upper and lower bounds for the effective properties of the composite, enabling a more accurate prediction of the mechanical behavior [28]. The Mori–Tanaka model and the Generalized Self-Consistent Model (GSCM) are both used for predicting the mechanical properties of composite materials with complex microstructures [26,27]. However, the Mori–Tanaka model is based on the assumption that the inclusions within the composite material are spherical while the GSCM is a more advanced model that can handle a wider range of inclusion shapes, sizes, and orientations. Each of these models has specific applications and assumptions, making them valuable tools for studying materials with multiscale structures and behaviors. Researchers choose the model that best suits the material and properties they want to analyze. The equations that are used in each of the models mentioned above are provided in Table 1 [29]. However, although these models can effectively predict the mechanical properties of multidimensional composite materials with inclusions, their applicability is restricted when it comes to complex structures. The models' limitations become more pronounced when dealing with intricate geometries, non-uniform distributions of inclusions, and interactions between inclusions. In such cases, more advanced models and numerical methods are needed to accurately predict the mechanical properties of complex composite structures. Research has identified that the main challenge in using Continuum-Based Micromechanical Models (CBMM) for asphalt materials is to accurately model the strengthening effect of particle contacts under conditions of high concentrations of fillers and elevated temperatures [30]. To effectively address this challenge, a comprehensive approach has been proposed that includes creating a realistic microstructure model, taking into account the physical mechanisms behind particle-contact stiffening, considering the viscoelastic behavior of the matrix material, and using DEM as a valuable numerical tool. Additionally, research indicates that existing micromechanical models fall short in accurately predicting the mechanical properties of porous asphalt mixtures such as Zeer Open Asphalt Beton (ZOAB), which is commonly used in the Netherlands due to its noise reduction properties, efficient water drainage, and resistance to rutting. Analysis of ZOAB suggests that this mixture may possess unique characteristics or microstructural features that call for a different modeling approach and more advanced models specifically designed to identify its properties.

To address the challenges in modeling complex mixtures like ZOAB, researchers have been exploring more sophisticated micromechanical approaches. In this context, the "Generalized Self-Consistent scheme" has been introduced as a novel concept [31]. This approach provides a more accurate depiction of these materials' behavior compared to the commonly employed Mori–Tanaka

scheme, especially when modeling materials with matrix-inclusion structures. Consequently, the selection of an appropriate method depends on the specific requirements of the investigation at hand.

3.2. Constitutive models

The transmission of information between multiple scales is also possible by the effective connection between ordinary differential equations (ODEs) and partial differential equations (PDEs) provided by finite element (FE) or discrete element (DE) techniques [32]. Once a solid understanding of the governing equations is achieved, these models can predict the behavior of a system based on the initial and boundary conditions, which are typically known at specific points.

However, the accuracy of these predictions relies on understanding the system's physics, including aspects such as kinematic equations and the principles of mass, momentum, and energy balance. To make accurate predictions, the constitutive equations that describe the system's behavior are also needed. These constitutive equations must be calibrated using experimental data or data generated through multiscale modeling [28].

In the case of bituminous mixtures, the viscoelastic behavior of the asphalt binder is particularly important. The Maxwell model is commonly used to represent this behavior. The Maxwell model consists of linear springs (elastic elements) and linear dashpots (viscous elements) as shown in Fig. 3. In the Maxwell model, the stress is decomposed into deviatoric and volumetric components as follows [33]:

$$S = 2G_0(e - \sum_{i=1}^{n} g_i e_i) \tag{7}$$

$$\sigma = 3K_0(e - \sum_{i=1}^{n} k_i e_i) \tag{8}$$

where S is the deviatoric stress, σ is the volumetric stress, G_0 and K_0 are the instantaneous shear and bulk moduli, respectively. g_i and k_i are the Prony series parameters, and e_i is the viscous strain in each Maxwell element. However, while the Maxwell model provides a foundational framework, for more comprehensive 3D numerical applications in viscoelastic materials like asphalt, a more detailed constitutive description is necessary [34]. In the general 3D case, the stress–strain relationship for a linear viscoelastic material can be expressed using the Boltzmann superposition principle as follows [35]:

$$\sigma_{ij}(t) = \int_0^t 2G(t-\tau)\frac{\partial e_{ij}(\tau)}{\partial \tau} d\tau + \delta_{ij}\int_0^t K(t-\tau)\frac{\partial \epsilon_{kk}(\tau)}{\partial \tau} d\tau \tag{9}$$

where σ_{ij} is the stress tensor, e_{ij} is the deviatoric strain tensor, ϵ_{kk} is the volumetric strain, $G(t)$ is the shear relaxation modulus, $K(t)$ is the bulk relaxation modulus, and δ_{ij} is the Kronecker delta. The relaxation moduli $G(t)$ and $K(t)$ can be represented as follows [35]:

$$G(t) = G_\infty + \sum_{i=1}^{n} g_i e^{-t/\tau_i} \tag{10}$$

$$K(t) = K_\infty + \sum_{i=1}^{n} K_i e^{-t/\tau_i} \tag{11}$$

where G_∞ and K_∞ are the long-term shear and bulk moduli, g_i and k_i are the Prony series coefficients, and τ_i are the relaxation times.

For numerical implementation, it is often convenient to use a recursive algorithm. The stress at time t_n can be expressed as [36]:

$$\sigma_{ij}(t_n) = 2G_\infty e_{ij}(t_n) + K_\infty \epsilon_{kk}(t_n)\delta_{ij} + s_{ij}^n + p^n\delta_{ij} \tag{12}$$

where s_{ij}^n and p^n are history variables that can be updated recursively.

In multiscale modeling of paving materials, two primary numerical methods are commonly employed to solve these constitutive equations:

FEM, based on continuum mechanics, discretizes the domain into elements and solves for nodal displacements using the principle of virtual work:

$$\int_\Omega \boldsymbol{\sigma} : \delta\boldsymbol{\epsilon}\, d\Omega = \int_\Gamma \mathbf{t}\cdot\delta\mathbf{u}\, d\Gamma + \int_\Omega \mathbf{f}\cdot\delta\mathbf{u}\, d\Omega \tag{13}$$

where $\boldsymbol{\sigma}$ is the stress tensor, $\boldsymbol{\epsilon}$ is the strain tensor, $\mathbf{t}$ is the traction vector, $\mathbf{f}$ is the body force vector, and $\delta\mathbf{u}$ is the virtual displacement. FEM excels in modeling complex geometries and is efficient for large scale problems, but can struggle with discontinuities and large deformations.

Conversely, DEM treats the material as discrete particles and models their interactions directly. The motion of each particle i is governed by Newton's second law:

$$m_i\frac{d^2\mathbf{x}_i}{dt^2} = \mathbf{F}_i \tag{14}$$

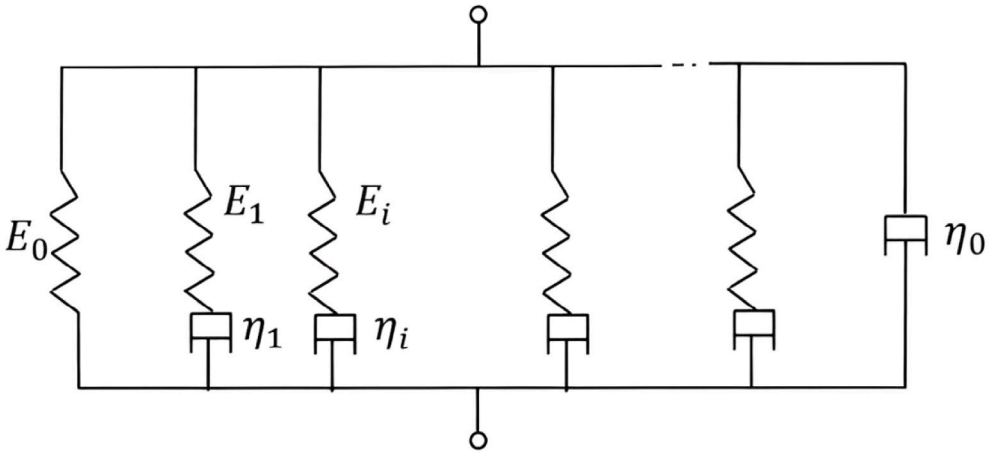

Fig. 3. Configuration of the Maxwell model: E_i = Springs; η_i = dashpots.

Table 2
Summary of Prony series optimization methods.

Reference	Method	Description	Key features
[37,38]	Levenberg–Marquardt	Iterative technique that locates a local minimum of a function	Efficient for nonlinear least squares problems; combines gradient descent and Gauss–Newton method
[39]	Genetic algorithms	Evolutionary algorithm inspired by natural selection	Uses mechanisms like mutation, crossover, and selection; good for global optimization
[40,41]	Particle swarm optimization	Population-based stochastic optimization technique	Inspired by social behavior of bird flocking or fish schooling; effective for high-dimensional problems
[42]	Hybrid Methods	Combination of two or more optimization techniques	Combines strengths of multiple methods; can overcome limitations of individual techniques

where m_i is the particle mass, $\mathbf{x}_i$ is the mass position, and $\mathbf{F}_i$ is the total force acting on it. DEM naturally handles particulate materials and discontinuities, but is computationally intensive for large systems. The choice between FEM and DEM depends on the specific aspects of the paving material behavior being modeled, with each method offering distinct advantages in different scenarios.

Regardless of the chosen numerical method (FEM or DEM), the accurate representation of material behavior through constitutive models often involves determining the parameters of the Prony series representation. Various optimization techniques were employed to determine these parameters (Table 2). One common approach is to minimize the error between the experimentally measured complex modulus and the predicted complex modulus [37]. The complex modulus can be expressed in terms of the Prony series parameters:

$$G^*(\omega) = G_\infty + \sum_{i=1}^{n} \frac{g_i(\omega\tau_i)^2}{1+(\omega\tau_i)^2} + i\sum_{i=1}^{n} \frac{g_i\omega\tau_i}{1+(\omega\tau_i)^2} \tag{15}$$

The optimization problem can be formulated as:

$$\min_{\{g_i,\tau_i\}} \sum_{j=1}^{m} \left(\frac{|G^*_{\text{exp}}(\omega_j)| - |G^*_{\text{pred}}(\omega_j)|}{|G^*_{\text{exp}}(\omega_j)|} \right)^2 + \left(\frac{\delta_{\text{exp}}(\omega_j) - \delta_{\text{pred}}(\omega_j)}{\delta_{\text{exp}}(\omega_j)} \right)^2 \tag{16}$$

where $|G^*_{\text{exp}}|$ and δ_{exp} are the experimentally measured magnitude of the complex modulus and phase angle, and $|G^*_{\text{pred}}|$ and δ_{pred} are the predicted values. Algorithm Algorithm 1 outlines the general procedure for determining Prony series parameters.

The Burger model expands upon the Maxwell model by incorporating an additional "dashpot-spring" element (Fig. 4). This parallel combination of spring and dashpot allows the Burger model to capture more complex viscoelastic behaviors [43]. The constitutive equation for the Burger model can be expressed as:

$$\epsilon(t) = \frac{\sigma_0}{E_1} + \frac{\sigma_0}{E_2}(1 - e^{-\frac{E_2}{\eta_2}t}) + \frac{\sigma_0}{\eta_1}t \tag{17}$$

where $\epsilon(t)$ is the strain, σ_0 is the applied stress, E_1 and E_2 are the elastic moduli of the springs, and η_1 and η_2 are the viscosities of the dashpots.

Algorithm 1 Determination of Prony Series Parameters

Require: Experimental data $\{(\omega_j, |G^*_{\text{exp}}(\omega_j)|, \delta_{\text{exp}}(\omega_j))\}_{j=1}^{m}$
Require: Number of Prony terms n
Ensure: Prony series parameters $\{g_i, \tau_i\}_{i=1}^{n}$ and G_∞
Initialize $\{g_i, \tau_i\}_{i=1}^{n}$ and G_∞
while not converged **do**
  for $j = 1$ to m **do**
    Compute $G^*_{\text{pred}}(\omega_j)$ using Eq. (8)
    Compute $|G^*_{\text{pred}}(\omega_j)|$ and $\delta_{\text{pred}}(\omega_j)$
  end for
  Compute error E using Eq. (9)
  if $E <$ tolerance **then**
    converged ← true
  else
    Update $\{g_i, \tau_i\}_{i=1}^{n}$ and G_∞ using chosen optimization method
  end if
end while
return $\{g_i, \tau_i\}_{i=1}^{n}$ and G_∞

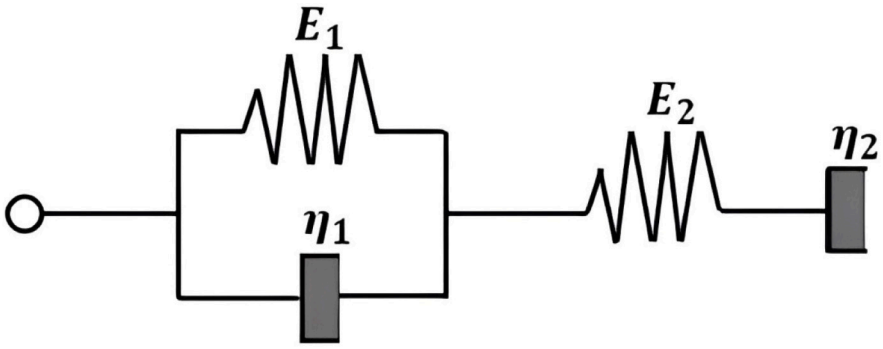

Fig. 4. Configuration of the Burger model: E_i = Springs; η_i = dashpots.

Other advanced models like Huet, Huet-Sayegh-Soleimani, and 2S2P1D have been developed to describe more complex viscoelastic behaviors [44,45]. For instance, the 2S2P1D model (2 Springs, 2 Parabolic elements, 1 Dashpot) is described by the following complex modulus:

$$E^*(\omega) = E_0 + \frac{E_\infty - E_0}{1 + \delta(i\omega\tau)^{-k} + (i\omega\tau)^{-h} + (i\omega\beta\tau)^{-1}} \tag{18}$$

where E_0 is the static modulus, E_∞ is the glassy modulus, τ is the characteristic time, k and h are exponents, δ is a dimensionless constant, and β is a parameter linked to the dashpot viscosity. Another important aspect that needs to be considered is the inclusions such as microscale fillers and mesoscale aggregates in viscoelastic models, which add a layer of complexity to the analysis of material behavior. These inclusions, often modeled as elastic materials, are characterized by their Poisson's ratio (ν) and Young's modulus (E). The effective properties of the composite can be estimated using techniques like the rule of mixtures:

$$E_c = E_m V_m + E_i V_i \tag{19}$$

where E_c, E_m, and E_i are the Young's moduli of the composite, matrix, and inclusions respectively, and V_m and V_i are their volume fractions.

More advanced homogenization methods for the accurate estimation of the effective properties are provided in Section 3.1

The interaction between inclusions and the matrix can be modeled using various approaches, including perfect bonding ("tie contact"), cohesive zone models for adhesive forces, or friction models for relative motion. These interactions significantly influence the overall behavior of the composite material and can be captured in FE analyses.

However, while these models provide valuable insights, it is crucial to validate them through experimental testing, as real materials may exhibit behaviors beyond the scope of simplified models. The choice of modeling approach depends on the specific material system and the required level of detail. More detailed examples of the applications of these models are in Section 4.1.

3.3. Phase field modeling (PFM) of bituminous mixtures

PFM is another robust computational method utilized for simulating the evolution of microstructures in various materials. This technique has been applied in numerous areas such as the crystallization process during a metal's solidification, transformations of solid-state phase, grain growth within materials, crack progression, and electromigration [46,47]. In the context of paving materials, PFM has been effectively used to study the evolution of microstructure and phase separation in polymer-modified bitumen (PMB). The fundamental principle of PFM is the use of a continuous order parameter ϕ to describe the spatial and temporal evolution of different phases or microstructural features [48].

The core of the PFM approach is the free energy functional, which for a binary system like PMB can be expressed as:

$$F[\phi] = \int_{\Omega} \left[f(\phi) + \frac{\kappa}{2} |\nabla \phi|^2 \right] dV \tag{20}$$

where $f(\phi)$ is the bulk free energy density, κ is the gradient energy coefficient, and Ω is the domain of interest. The gradient term $\frac{\kappa}{2}|\nabla\phi|^2$ penalizes sharp interfaces, leading to a diffuse interface description characteristic of PFM.

The temporal evolution of the order parameter is typically described by the Cahn-Hilliard equation [49]:

$$\frac{\partial \phi}{\partial t} = M \nabla^2 \left(\frac{\delta F}{\delta \phi} \right) \tag{21}$$

where $M(\phi)$ is the mobility function and $\frac{\delta F}{\delta \phi}$ is the functional derivative of the free energy with respect to ϕ.

Several studies have investigated the microstructure evolution in PMB systems [50,51]. The following form for the bulk free energy density was proposed:

$$f(\phi) = A\phi^2(1-\phi)^2 + B\phi(1-\phi) \tag{22}$$

where A and B are parameters related to the interaction energy between the polymer and bitumen phases. This model successfully captured the formation of polymer-rich domains within the bitumen matrix and demonstrated how factors such as polymer concentration and temperature affect the phase separation process.

Beyond PMB, PFM has also been applied to study other aspects of bituminous mixtures. For example, it has been employed to model low-temperature cracking in asphalt binders [52]. This model integrates the viscoelastic properties of the binder with the fracture process, offering valuable insights into the mechanisms of crack initiation and propagation. The applications of PFM are discussed in detail in Section 4.1.

3.4. Artificial neural networks (ANNs)

The perceptron, which was first introduced by Rosenblatt, (1958), served as the basis for early ANNs, was designed as a binary classifier and was based on a simplistic model of the biological neuron [53]. The basic idea was to receive inputs, process them, and produce an output (0 or 1). The perceptron was trained by strengthening the weights of connections that lead to correct predictions and weakening those that do not contribute to the predictions. The perceptron computes a weighted sum of the input features as follows:

$$z = w_1 x_1 + w_2 x_2 + \cdots + w_n x_n = \sum_{i=1}^{n} w_i x_i \tag{23}$$

where, x_i represents the input features, w_i are the corresponding weights, and n is the number of input features. The perceptron uses an activation function to make a decision (classification). The perceptron is trained using the perceptron learning rule, which updates the weights based on the errors made in predictions. The weight update rule is given by:

$$w_i \leftarrow w_i + \Delta w_i \tag{24}$$

$$\Delta w_i = \eta(t-y)x_i \tag{25}$$

where Δw_i is the change in the weight, η is the learning rate (a small positive constant), t is the true label, and y is the predicted label. This update is performed for each weight (w_i) and is repeated for all training examples. However, the major limitation of the original perceptron was its inability to solve problems that are not linearly separable.

ANNs represent a dynamic and expanding field within artificial intelligence (AI) that has influenced numerous sectors due to their ability to solve complex and nonlinear problems [54]. ANNs have experienced significant evolution since their origin, taking inspiration from the perceptron and human nervous system. Modern ANNs, especially deep learning networks, consist of multiple layers of neurons. These layers include hidden layers between the inputs and outputs. Unlike the simple learning rule of the perceptron, modern ANNs use more sophisticated algorithms such as backpropagation. This allows them to learn from errors in a more nuanced way and adjust weights throughout the network.

In a basic ANN, each neuron computes a weighted sum of its inputs. For a neuron j in layer l, the weighted sum $z_j^{(l)}$ is computed as:

$$z_j^{(l)} = \sum_{i=1}^{n} w_{ji}^{(l)} x_i^{(l-1)} + b_j^{(l)} \tag{26}$$

where, $w_{ji}^{(l)}$ are the weights connecting neurons i in layer $l-1$ to neuron j in layer l, $x_i^{(l-1)}$ are the outputs from the previous layer (or input features for the first hidden layer), and $b_j^{(l)}$ is the bias term of neuron j in layer l. Each neuron's output is typically passed through a non-linear activation function. Common activation functions include the sigmoid, tanh (hyperbolic tangent), and ReLU (Rectified Linear Unit). The output $a_j^{(l)}$ of neuron j is:

$$a_j^{(l)} = f(z_j^{(l)}) \tag{27}$$

where f is the activation function. The final layer's output depends on the specific task (e.g., classification, regression). For classification, a softmax function is often used in the output layer. The network's performance is evaluated using a loss function, such as mean squared error (MSE) for regression or cross-entropy loss for classification. The network learns by adjusting the weights to minimize the loss. This is done using the backpropagation algorithm, which computes the gradient of the loss function with respect to each weight in the network, and then updates the weights in the direction that reduces the loss. The weight update rule is:

$$w_{ji}^{(l)} \leftarrow w_{ji}^{(l)} - \eta \frac{\partial \text{Loss}}{\partial w_{ji}^{(l)}} \tag{28}$$

where η is the learning rate. During training, the network undergoes a forward pass where inputs are fed through the network to produce an output. Then, a backward pass is conducted using backpropagation to compute the gradient of the loss function and update the weights.

Modern ANNs can tackle a vast array of complex tasks, including image and speech recognition, natural language processing. As a result, researchers have categorized ANNs into three main types based on their network structure.

The first type is the Multi-Layer Perceptron Neural Network (MLPNN), which consists of at least three layers: an input layer, an output layer, and one or more hidden layers. Each layer is fully connected to the next, allowing MLPNNs to learn non-linear models. They can be applied to both classification and regression tasks [55]. The backpropagation algorithm used for training enables them to learn from errors and adjust weights throughout the network [56].

The second type is the Recurrent Neural Network (RNN), which processes sequential data by using the output from the previous step as input for the current step. This gives RNNs a form of memory, making them useful for tasks such as speech recognition, natural language processing, and time-series prediction [57,58]. In multiscale modeling, this method has been widely used when the loading rate/path impacts the outputs [53,54]. The basic equations for an RNN can be written as follows:

$$h_t = f(W_{hh} h_{t-1} + W_{xh} x_t + b_h) \tag{29}$$

$$y_t = W_{hy} h_t + b_y \tag{30}$$

where h_t is the hidden state at time t, x_t is the input at time t, y_t is the output at time t, W_{hh}, W_{xh}, W_{hy} are weight matrices, b_h and b_y are bias vectors, and f is an activation function. Fig. 5 illustrates the structural differences and typical applications of MLPNNs and RNNs in paving materials.

The third type is the Convolutional Neural Network (CNN), which is particularly effective at processing images and videos. CNNs use a series of convolutional and pooling layers to extract features from input data, which the network then uses to classify the input or make predictions [59]. CNNs are designed to learn spatial hierarchies of features from the input data in an automatic and adaptive way. For example, they can be used to identify pavement distresses such as cracking and disintegration [60]. The main operation in a CNN is the convolution, which can be represented as:

$$(f * g)(x, y) = \sum_i \sum_j f(i, j) \cdot g(x - i, y - j) \tag{31}$$

where f is the input, g is the kernel or filter, and (x, y) are the coordinates in the output feature map. Additionally, the pooling operation, often used in CNNs, can be represented as:

$$\text{pool}(x) = \max(x_i) \text{ or } \text{avg}(x_i) \tag{32}$$

where x_i are the values in a local region of the feature map. However, CNNs are not within the scope of this study. ANNs are believed to be superior to conventional multiscale methods as the data obtained from lower scale computations are utilized to predict the behavior of materials. These data are adjusted and converted into material datasets to accurately depict the material's properties [57,61].

In materials science, the accurate prediction of materials performance is essential for enhancing their quality and minimizing environmental and safety risks [62]. Complex, high-dimensional datasets with nonlinear relationships often pose significant challenges for traditional regression techniques. This is especially true when the behavior of the data changes across different scales, making it difficult for conventional models to capture the full range of patterns and interactions present. This has prompted the integration of ANNs into multiscale modeling frameworks. ANNs excel at detecting complex patterns within extensive datasets that span from the molecular to the macroscopic scale [63]. Training ANNs with data from these scales allows for precise predictions of how materials respond under various conditions, thereby addressing the limitations of traditional methods and resulting in more robust and reliable material performance predictions. More detailed examples of the applications of ANNs are in Sections 4.2 and 4.4.

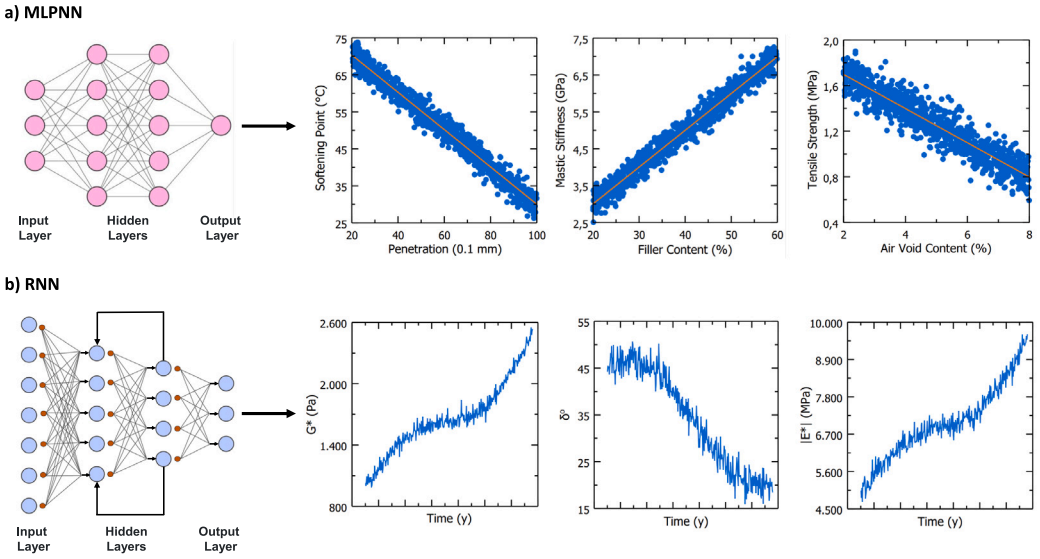

Fig. 5. ANN architectures for predicting paving material properties with outputs examples of each case: (a) MLPNN, and (b) RNN.

4. Multiscale modeling of bituminous mixture

4.1. Modeling the response of asphalt binders and mastics

Asphalt binder, commonly referred to as bitumen, is characterized by its viscoelastic nature. This denotes a combination of both elastic solid and viscous liquid behaviors. The properties of asphalt binder are significantly influenced by various factors, including the conditions under which it is tested in the laboratory (such as temperature and frequency) and the aging processes it undergoes. The chemical complexity of bitumen and the variability in its properties make it an interesting subject of study. It plays a crucial role in determining the behavior of the other scales (mastic, mortar, mixture). To simulate the mechanical characteristics of asphalt binder in a FE or DE model, certain parameters are needed. These include the Young's Modulus and Poisson ratio, which characterize the elastic response, along with parameters derived from models such as the Maxwell model (Prony Series Parameters) [64]. These parameters should be calibrated based on experimental tests such as the dynamic shear rheometer test (DSR), and three-point bending test. The temperature can also be set using parameters from the WLF equation. For example, ABAQUS allows the WLF equation to be used at any convenient temperature, other than the glass transition temperature, as the reference temperature. The form of the equation remains the same, but the constants are different [33].

Efforts have been made to integrate the time-dependent characteristics of bitumen into numerical simulations. For example, the Burger model has been utilized within a DE framework to simulate the DSR tests on a bitumen sample across a frequency range of 0.01 to 10 Hz [43]. The mechanical behavior of bituminous mastic has also been modeled using both Burger and Maxwell models. One approach incorporated the Burger model into a DEM framework to investigate how changing the proportions of cement and limestone filler in a bitumen emulsion mixture affects its rutting resistance under temperature variations and repeated stress [65]. Another study employed the Maxwell model within a FE model to examine the behavior of mastic with different filler types [66]. Additionally, a preliminary PFM was developed to study the evolution of microstructure in a mixture comprising SARA fractions [67]. This model revealed a separation between high and low polar fractions (asphaltenes and saturates) and the formation of a bee structure, which is considered to be a weak point where cracks may initiate and propagate.

The bee phase is also believed to be a phase-separated from the bulk of the bitumen and blooms to the surface of the bitumen due to the low surface free energy of the wax [68]. Table 3 summarizes some studies on asphalt binder performance prediction using FE and DE models.

However, it is crucial to note that these models have not been extensively evaluated under extreme conditions such as high frequencies, temperatures, or varying loads. Consequently, the behavior of these models may vary when subjected to different loading tests, such as linear sine sweep tests or log sine sweep tests. Moreover, the models' responses under various aging conditions have not been compared in existing studies. Aged bitumen usually becomes more elastic, which could potentially yield different results compared to the GSCM [69,70]. The GSCM assumes a certain level of homogeneity and consistency in the material properties. However, when bitumen ages, it undergoes physical and chemical changes that can alter its properties. To tackle this problem, a sensitivity analysis specifically designed for these conditions, using FE/DE models, different loading tests, and aging conditions, is suggested. Additionally, while some studies investigated two different volumetric percentages of fillers within bitumen, illustrations of how the rheological properties change with varying frequencies for different filler percentages are still not clear [65]. It is expected that the response of the mastic at low frequencies remains consistent for different filler percentages, with differences primarily

Table 3
Overview of published FE and DE models for asphalt binder and mastic.

Reference	Method	Material	Model	Analysis
[43]	DEM	Binder	Burger	Mechanical response under different frequencies
[76]	FEM	Binder	Maxwell	New fatigue test
[65]	DEM	Mastic	Burger	Different types of fillers to bitumen ratio
[66]	FEM	Mastic	Maxwell	Different types of fillers
[77]	FEM	Mastic	Maxwell	Response under different frequencies
[78]	FEM	Mastic	Burger	Response when adding sunflower oil as a modifier
[67]	FEM	Binder	PFM[a]	Separation of SARA fractions
[50,79]	FEM	Polymer-Modified Bitumen	PFM[a]	Polymer separation at various temperatures and conditions
[80]	FEM	Binder	PFM[a]	Fracture failure in crack interaction of Asphalt Binders at Low Temperature
[81]	FEM	Mastic	2S2P1D[b]	Asphalt-filler interaction

[a] PFM refers to the Phase Field Method.
[b] Model consists of combinations of two springs , two parabolic elements and one dashpot.

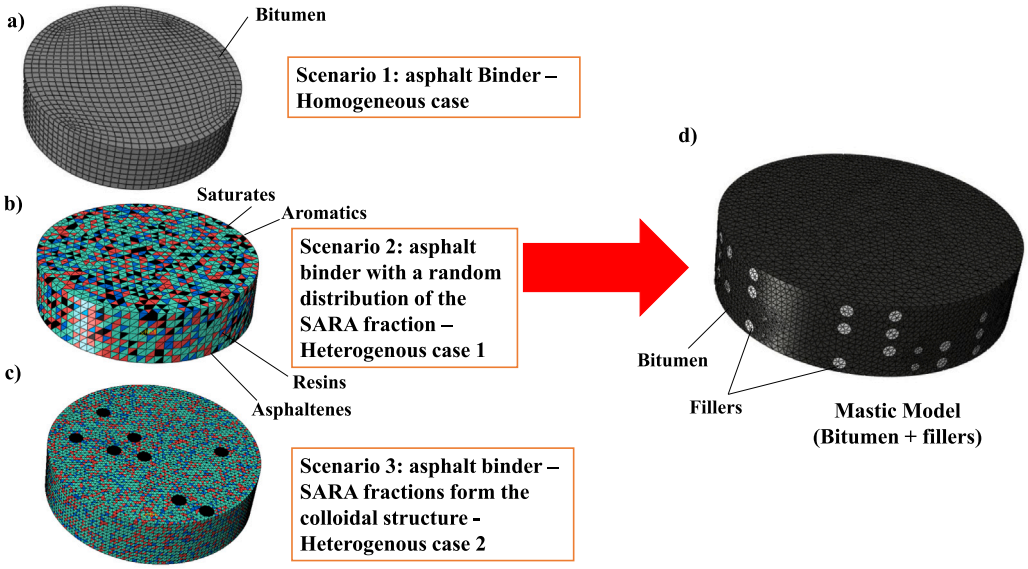

Fig. 6. Potential approaches for incorporating SARA fractions into FE models.

appearing at higher frequencies where the mastic becomes more elastic. Furthermore, beyond mechanical loads, to the best of the author's knowledge, there are currently no numerical aging models at the binder/mastic scale that can replicate laboratory aging conditions. Moreover, the complexity of asphalt binder presents a significant challenge in developing numerical models that can accurately link its chemical composition to its mechanical behavior [71]. Fig. 6 demonstrates possible strategies for integrating SARA fractions into FE models while also indicating a larger scale (mastic scale). Three scenarios are presented. In the first scenario (Fig. 6a), a basic homogeneous situation is proposed. The second scenario suggests a random distribution of SARA fractions in the matrix inspired by [13] (Fig. 6b). The third scenario presents a concept of colloidal structure, where asphaltenes and resins create micellar chains that are surrounded by saturates and aromatics, indicating a more intricate interaction within the bitumen matrix (Fig. 6c). The properties of the SARA fractions, which need to be implemented in these model (i.e., Prony series parameters), can be determined by first separating the SARA fractions and then individually testing each fraction using the DSR test [72,73]. An upscaling can be performed to the mastic by introducing spheres (treated as an elastic substance) into the matrix, and a sensitivity analysis can be performed (Fig. 6d). In a similar approach, two scales models were developed to estimate the elastic properties of shales at the core scale (fine-grained, laminated sedimentary rocks consisting of silt- and clay-sized particles) [8,74]. In these models, solid grains representing minerals were randomly distributed based on their volume fraction and elastic properties to form different types of shales [75].

This methodology could potentially be applied at the binder scale. However, it is critical to consider that the SARA fractions are viscoelastic materials, unlike the elastic materials such as solid grains. Therefore, the implementation of this methodology requires careful consideration.

Table 4
ANNs models of asphalt binder and asphalt mastic: T = test temperature; f = test frequency; G' = storage modulus; G'' = loss modulus; η = viscosity; G_c = different geopolymer concentration; FAR = filler-asphalt ratio; G_r = five gradation components, V_b = base binder viscosity; C_t = compaction temperature; AV = air voids percentage; ITS = indirect tensile strength; and SBS = Styrene butadiene styrene.

Reference	Material	Input parameters	Predicted parameters
[84]	Binder	T, f, G', G'', η	Recovery and nonrecoverable compliance
[85]	Modified Binder	f, T, G_c	Complex shear modulus
[86]	Mastic	T, f, FAR	Complex shear modulus
[87]	Binder	T, f, G_r, V_b	Rutting performance parameters
[88]	Binder	C_t, AV, ITS	Degree of binder activity
[89]	SBS Modified Asphalt	ATR-FTIR data	SBS content, needle penetration, softening point

4.2. Applications of ANNs in asphalt binder and mastic performance prediction

The complex behavior of asphalt binder and mastic under various conditions suggests that traditional analytical models may not be sufficient for accurate predictions. In addition, FE and DE models may also fall short due to their inability to incorporate all the parameters that influence the behavior of these materials. This is where ML can provide significant value, as it excels at identifying complex patterns and relationships within large datasets [82]. Various ML algorithms have been employed to predict properties across different scales of bituminous and modified bituminous mixtures [83]. However, the majority of research has concentrated on using ANNs due to their robust capability to model complex, non-linear relationships within the data. These studies have sought to create models capable of precisely predicting the mechanical properties of asphalt mixtures, including strength and durability, using inputs like mixture composition, temperature, and age. Nevertheless, the implementation of these models at the binder scale remains constrained by the limited availability of extensive datasets that cover the wide range of parameters influencing its properties.

To illustrate this point, a study developed an ANN model capable of predicting recovery and nonrecoverable compliance of asphalt binder at high stress [84]. The model used five input parameters: test temperature, test frequency, storage modulus, loss modulus, and viscosity. The high accuracy of the predictions suggests that such models could be valuable in designing asphalt mixtures that perform optimally under various conditions.

In another study, an ANN model was established to predict the performance of geopolymer modified asphalt binder [85]. The research tested different combinations of parameters, algorithms, and network architectures, and identified the best performing model based on statistical measures. The results highlighted not only the potential of ANNs in predicting complex material behaviors but also the significance of choosing the right model architecture and training algorithm for accurate predictions. Moving beyond the asphalt binder scale, research has also shown how ANNs can predict G^* of asphalt mastic samples using input parameters such as temperature, frequency, and filler-asphalt ratio [86]. This study demonstrated that ANN models can be a useful and efficient tool for evaluating the material properties of asphalt mastic. Table 4 provides a summary of various studies focusing on the prediction of asphalt binder/mastic using ANNs models.

However, while the use of ANNs in predicting the characteristics of asphalt binder and mastic shows great potential, the main issue is the lack of extensive datasets that cover all the parameters affecting these materials' behavior. For example, there is a significant gap in research that includes crucial factors such as SARA fractions and essential physical properties such as penetration and softening point. These factors are critical in understanding asphalt binder and mastic and can greatly influence their performance under various conditions. Moreover, despite the demonstrated potential of ANNs, there is still a need for an exhaustive comparative study that investigates various algorithms and methodologies to identify the most impactful parameters on these materials' properties and determine which ANN architectures and training algorithms provide the most precise predictions. Integrating all these methods could lead to more accurate and flexible predictive models for asphalt binder and mastic behavior, addressing the complex and varied nature of these materials.

Fig. 7 proposes a multiscale methodology that utilizes ANNs to establish a connection between input variables and rheological characteristics like G^* and δ. The ANNs are then used to identify the most impactful features that affect these properties. The analysis begins at the binder level, taking into account aspects such as aging conditions, chemical composition, and physical properties. The process then progresses to the mastic level, where the model's complexity and accuracy are improved by incorporating additional properties, specifically the percentage of filler and stiffness. This approach allows ANNs to integrate these elements, providing a thorough evaluation of the material's behavior.

4.3. Applications of numerical simulations in asphalt mortar and mixture

When shifting from modeling asphalt binder and mastic on their own to modeling them in the context of mortar and mixture, it is notable that a broader range of studies becomes available [90]. This can be attributed to the practical importance, complexity, engineering challenges associated with asphalt mixtures, and the availability of data and the growing interest in infrastructure applications. Building on this, modeling asphalt mixture behavior involves a blend of mechanistic principles, empirical relationships, numerical simulations, and statistical methods. These models are not isolated; they draw upon data from various sources, including material characterization, traffic data, climate data, and laboratory tests. For example, a FE model was built to assess the fatigue behavior of asphalt mortar under repeated loading over time [91]. This work found that voids negatively affect the fatigue performance of asphalt mixtures, with damage primarily starting at the edges of voids and significantly increasing as the void

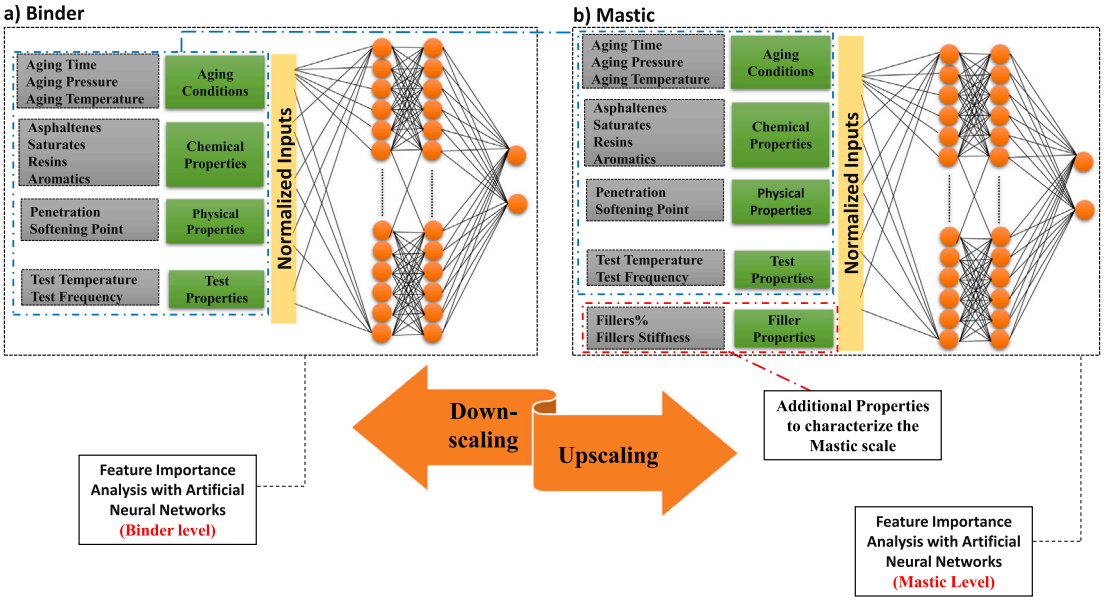

Fig. 7. Upscaling analysis approach from binder level to mastic level using ANNs.

ratio rises. In another study, a multiscale FE model of asphalt mixture was created to understand the cracking mechanisms in asphalt mixtures [92]. This comprehensive model considered asphalt mixtures as two separate phases: asphalt mortar and aggregates. It explored various factors influencing cracking and highlighted performance differences between different asphalt mixtures. Additionally, a FE model was developed to predict crack propagation, branching, and coalescence in asphalt mixtures, shedding light on how cracks evolve in asphalt concrete [93].

Furthermore, advanced FE models for predicting how asphalt pavement materials behave under different conditions have been proposed, with a focus on understanding their microstructure and incorporating damage-coupled viscoelastic behavior into the models [9]. Moreover, a 3D microstructural numerical model has been developed that combines the viscoelastic properties of the asphalt mortar and the elastic properties of aggregates to predict how the material responds to triaxial loads within a linear viscoelastic range [94,95].

However, researchers have not limited their investigations to understanding how asphalt mortar and asphalt mixtures react to mechanical loads such as stresses and strains. In fact, they have made significant efforts to develop models for heat conduction, oxygen, and moisture diffusion within asphalt mixtures. These research are valuable because they help predicting the performance of pavements under varying environmental conditions, which ultimately affects the pavement's service life [96–98].

For instance, porous asphalt concrete (PAC) has been found to have distinct thermal properties compared to dense-graded asphalt mixtures due to the presence of interconnected air voids [99]. Another study proposed a FE model to predict the mechanical properties of asphalt mixtures, considering the mastic and aggregates as the main components [7]. Expanding on this approach, detailed microscale modeling has been combined with macroscopic simulations to understand how moving wheel loads affect asphalt pavement structures under various conditions [100]. This type of research offers a broader perspective on pavement performance. To further enhance the efficiency and accuracy of these simulations, a novel approach has been proposed to accelerate numerical simulations by combining neural networks with physics-based knowledge from classical material modeling [101]. This approach aims to address the challenges associated with purely data-driven surrogate models and shows promise in accurately predicting material behavior, even in scenarios not explicitly seen during training.

Building upon these advancements, researchers have developed more specialized models to address specific aspects of asphalt mixture performance. For example, a FE model has been introduced that captures the impact of aging and moisture damage on the performance of asphalt mixtures. This model serves as a foundation for incorporating other damage mechanisms in asphalt mixtures, such as fatigue or permanent deformations caused by a combination of environmental and loading conditions [102]. In another study, an equation-based model has also been proposed to capture the aging behavior of asphalt pavement [14]. However, even though this research is essential for advancing the understanding and design of road construction materials, there remains a lack of clarity regarding how properties transition from the nanoscale to the mesoscale and how the mechanical properties at each scale affect the subsequent one. Table 5 summarizes some studies on asphalt mortar/mixture performance prediction using numerical models.

Nevertheless, despite the extensive body of research available, the precise prediction of asphalt mixture behavior faces several notable challenges. On one hand, asphalt materials exhibit nonlinear behavior, which makes it difficult to predict their performance accurately. The relationship between stresses, strains, and other mechanical properties can change significantly under different loading conditions and scenarios [112,113]. On the other hand, environmental conditions such as UV radiation, freeze-thaw cycles,

Table 5
Overview of published FE and DE models for asphalt mortar, mixture.

Reference	Method	Material	Analysis
[91]	DEM	Mortar	Fatigue conditions
[76]	FEM	Mixture	Crack initiation in asphalt mixture
[65]	FEM	Mixture	Damage within asphalt mixture
[77]	FEM	Mortar	Response under shear load
[94,95]	FEM	Mixture	Response under a triaxial load
[103–105]	FEM	Mixture	Moisture diffusion
[99]	FEM	Mixture	Thermal conductivity
[106]	DEM	Mixture	Behavior during the compaction process
[107]	DEM	Mixture	Effects of aggregate on permanent deformation
[108]	FEM	Mixture	Predict the complex modulus and creep stiffness
[109]	DEM	Mixture	Micromechanical behavior evolution
[110]	FEM	Mixture	Effect of the interfacial zone on the tensile-damage behavior
[111]	DEM	Mixture	Effect of rejuvenator-modified mastic on asphalt mixture stiffness
[14]	FEM	Pavements	Oxidative aging of asphalt pavements

and chemical exposure contribute to the deterioration of asphalt mixtures over time. Modeling the long-term effects of these factors is challenging. Additionally, achieving a detailed simulation of asphalt mixtures often demands the utilization of advanced numerical methods and substantial computational resources, rendering it both computationally intensive and time-consuming. Consequently, alternative techniques are sought for improved solutions.

4.4. Application of ANNs in asphalt mortar and mixture

ANNs have been effectively utilized in predicting various properties of asphalt mixtures, including mechanical properties such as tensile strength, flexural modulus, and durability properties like resistance to rutting and abrasion. The availability of data for training ANNs is generally higher for asphalt mixtures compared to asphalt binder and mastic, given the large-scale production and usage of these mixtures. For instance, an ANN has been developed to predict the impact of aging on asphalt mixture properties using asphaltenes as the performance indicator [114]. This work highlighted the power of neural networks in identifying the nonlinear correlations between the mixture aging index (AMI) and other input factors. In another study, deep convolutional neural networks (DCNNs) with six convolution blocks have been utilized to determine the dynamic modulus (E^*) [115]. This model outperformed linear regression models in terms of prediction accuracy, thereby reducing the laboratory efforts required to measure E^* of asphalt mixture. Additionally, global sensitivity analysis revealed that certain parameters related to aggregates, binders, and mixture properties significantly impact E^* predictions [116]. Beyond predicting mechanical properties of asphalt mixtures, ANNs have also been employed to predict the rutting depth of asphalt pavement [117]. The proposed model is employed to analyze and rank the relative influence of the different model inputs on rutting depth. This wide range of applications showcases the ability and effectiveness of ANNs in this field. Table 6 summarizes some studies on asphalt mixture performance prediction using ANNs models.

However, the main limitation when using ANNs to predict properties of asphalt mixture is the quality of the data used to train the models and their ability to perform on unseen data. This is especially important when dealing with datasets related to factors such as traffic patterns, climate, and environmental conditions, which can show variability depending on the specific dataset in use. Furthermore, just as with the binder and mastic scale, relying solely on one technique to identify the factors influencing the dynamic modulus is not advisable. Different algorithms yield different results, thereby it is essential to analyze and compare results obtained from different algorithms to identify patterns and develop the most effective models. This allows researchers and industry professionals to focus their data collection efforts on the most critical factors affecting asphalt mixture properties.

5. Integration of scales and information: addressing limitations and mapping future directions

To create reliable models of bituminous mixtures, it is crucial to adopt a multiscale strategy that merges data and insights from various levels of detail from the behavior of asphalt binder at the nanoscale to the overall performance of pavements at the macroscale [124]. This process involves a combination of laboratory experiments, computational modeling, data integration, and validation, with an iterative feedback loop that enables continuous refinement and enhancement of the models as new data and insights emerge. The integration between different scales can be achieved through the following steps:

1- Nanoscale level: this level focuses on the behavior of the asphalt binder, which acts as the adhesive that binds the mixture. Understanding the rheological properties, aging protocols, and temperature-dependent behavior of the binder is essential. Additionally, the chemical composition of the binder significantly influences its overall behavior and should not be disregarded.

2- Microscale level: this level investigates the interaction between fillers and the asphalt binder. Despite numerous studies on filler impact on mastic performance, there is still ambiguity about the specific nanoscale factors that significantly influence both mastic and asphalt mixture behavior and their contribution to overall performance.

3- Macroscale level: while it is recognized that aggregate distribution, size, and shape have a significant effect on asphalt mixture behavior, how information from smaller scales influences this behavior remains unclear.

Table 6
ANNs models of asphalt mortar and asphalt mixture: T = temperature; f = frequency; AI = asphaltene aging index; VMA = voids in aggregates; AV = air voids; AG = aggregate gradation; MV = mixture volumetric; BP = binder properties; LF = loading frequency; TP = test parameters; η = viscosity; ABP = asphalt binder parameters; AP = aggregate percentage; EAC = effective asphalt content; $VPMA$ = voids percentage in aggregates; VFB = voids filled with binder; CV = contact volume; TC = traffic climate; ACL = AC layer; BL = base layer; SL = subgrade layer parameters; MT = mixture type (SMA, HMA); $Tech$ = technology (warm, hot); DSM = dynamic shear modulus of binder; BPA = binder phase angle, CPR = cumulative percent retained on different sieve sizes; $PP200$ = percent passing no. 200 sieve; PA = percentage of air voids in the mix; VEB = volumetric effective binder content; PPM = physical properties mechanical; MPM = properties gradation of the aggregate blend; GAB = bitumen content; BC also refers to bitumen content; $MMMD$ = marshall mix design parameters; PRB = percentage of rubber in the binder; $PRAP$ = percentage of RAP in the mixture; IF = initial flexural strain; VFA = percentage of voids filled with asphalt binder; IMS = initial mix stiffness; R_b = the percentage of rubber in the binder; R_p = the percentage of RAP in the mixture; ϵ = initial flexural strain; VFA = Volume of Voids filled with asphalt binder; S = initial mix stiffness; AGS = aggregate gradation sieves; VB = volume of binder, $EPVMA$ = effective percentage of voids in mineral aggregate; BSG = bulk specific gravity; $TMSG$ = theoretical maximum specific gravity; RAS = recycled asphalt shingles; RAP = recycled asphalt pavement; ABR = asphalt binder replacement; $PMAC$ = polymer modified asphalt concrete content; BG = binder grade; NOG = number of gyrations; PL = pavement layer; $ACMD$ = asphalt concrete mix design properties.

Reference	Asphalt material	ANNs input parameters	Predicted parameters
[114]	Mixture	T, f, AI, VMA, AV	Aging index
[115]	Mixture	AG, MV, BP, LF	Dynamic modulus
[116]	Mixture	$TP, \eta, ABP, AP, AV, EAC, VPMA, VFB, CV$	Dynamic modulus
[117]	Mixture	TC, ACL, BL, SL	Rutting depth
[118]	Stone Mastic Asphalt	$MT, Tech, f, T$	Dynamic modulus
[119]	Hot Mix Asphalt	$DSM, BPA, CPR, PP200, PA, VEB$	Dynamic modulus
[120]	Mixtures	Inputs representing the percentages passing from different sieves	Optimum asphalt content in asphalt mixture
[121]	Mixtures	$PPM, MPM, GAB, BC, MMMD, PRB, PRAP, IF, VFA, IMS$	Mix design
[122]	Mixtures	$R_b, R_p, \epsilon, VFA, S$	Fatigue life
[123]	Concrete	$AGS, VB, EPVMA, AV, BSG, TMSG, RAS, RAP, ABR, PMAC, BG, NOG, PL, ACMD$	Mix design

Researchers need to employ a variety of laboratory tests, computational models, and ML algorithms to investigate the different scales and to optimize the ultimate performance of asphalt mixture. An example of this is highlighted in [125], which pointed out that oxidative aging significantly impacts the properties of asphalt binder. However, these changes do not directly translate to similar changes in the modulus of asphalt mixtures. Therefore, more advanced models are required to predict how the aging of asphalt binder influences the modulus of asphalt concrete mixtures. Another example comes from findings that adding fibers to asphalt binders enhances their performance at high temperatures and increases their resistance to deformation [126]. The fiber-modified asphalt binders showed less penetration and a higher softening point, indicating better resilience to temperature changes and deformation. Fig. 8 shows a suggested multiscale FE/ML framework of bituminous mixture that address these issues. This framework shows a detailed process for collecting and analyzing data, applying ML models, and using FE analysis to interpret the results of the bituminous mixture. This framework also suggests the use of SHapley Additive exPlanations (SHAP) algorithm which uses a trained ANN to identify the most influential factors affecting the outputs. This is a significant advantage over traditional statistical methods such as Analysis of Variance (ANOVA) and Chi-Square tests. Traditional methods like ANOVA and Chi-Square tests rely on certain assumptions about the data while SHAP uses game theory to attribute the contribution of each feature to the prediction for each individual observation [127].

To further enhance the accuracy and efficiency of the multiscale approach, the use of physics-informed neural networks (PINNs), which combine the power of deep learning with the physical laws governing the behavior of the material, can be used [107,109,128]. PINNs are specialized neural networks that combine the power of ML with the governing physics equations, and they can play a pivotal role in enhancing the understanding and optimization of bituminous mixtures.

One of the primary advantages of PINNs is their ability to incorporate the known physical principles and equations governing bituminous mixtures into the ML framework. These physical principles, which describe the behavior of asphalt binders, fillers, and aggregates at different scales, can be challenging to capture accurately through traditional empirical data alone. Incorporating these principles into the neural network architecture ensures that the models adhere to the laws of physics, resulting in more accurate and physically meaningful predictions. Fig. 9 shows a proposed PINN framework designed to simultaneously solve three interlinked PDEs which are crucial in the study of bitumen aging. These equations model the diffusion of temperature (T), oxygen (P) and the formation of the carbonyl area (CA), which is a critical indicator of aging in bitumen materials. While traditional methods such as FEM, as applied in the research by [14], have been the standard for solving such complex PDEs, the emergence of PINNs brings several advantages. Unlike FEM, which requires extensive computational resources and can be time-consuming especially when dealing with nonlinear, transient, or multi-physical problems, PINNs introduce a more efficient approach. The efficiency of PINN in the automatic differentiation makes it possible to encode the PDEs as part of the learning process [129]. This results in a flexible and highly adaptive model that can predict the complex behaviors of bitumen aging with remarkable accuracy and significantly reduced computational cost. The proposed PINN can be upscaled to the mastic level or mixture level after incorporating the additional properties (fillers, aggregates). More detailed examples can be found in [130–135]. However, while PINNs have shown promise in various applications, they still face limitations, including occasional inaccuracies in predictions. These challenges underscore the need for further research to enhance their performance and reliability [130,136].

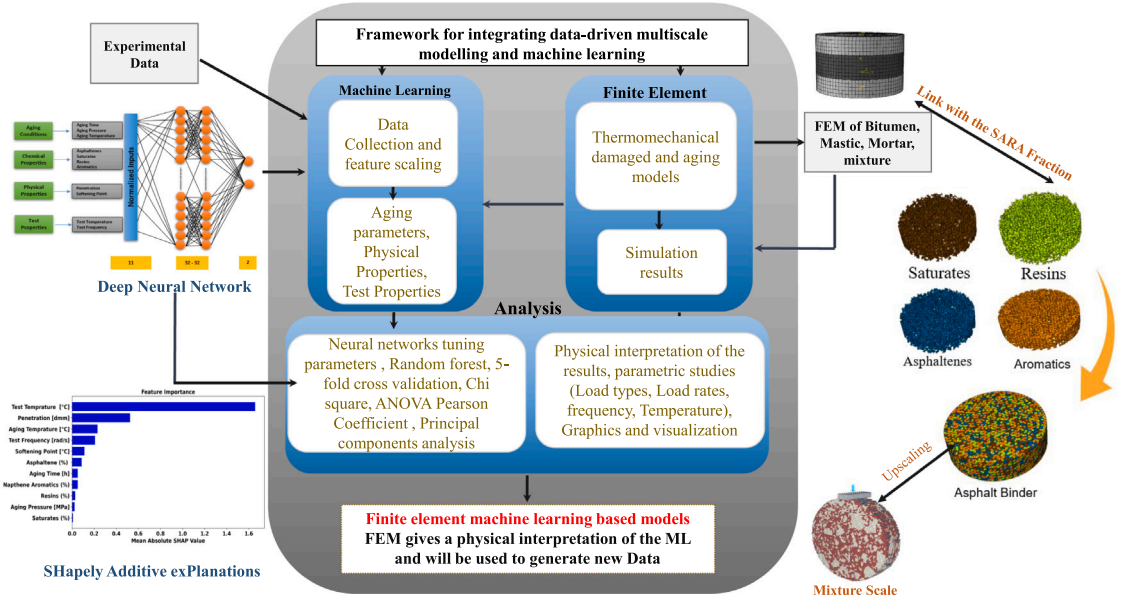

Fig. 8. Multiscale FE-ML framework of asphalt mixture.

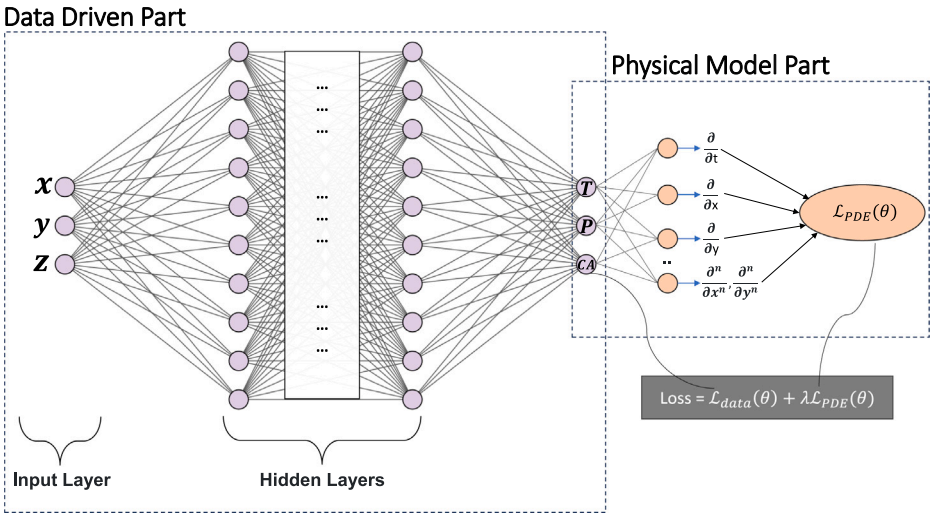

Fig. 9. PINN architecture to solve three interrelated 2D PDEs that model temperature diffusion T, oxygen diffusion P, and carbonyl area—an indicator of bitumen aging CA. $\mathcal{L}_{\text{data}}(\theta)$ represents the data-driven loss based on known measurements, $\mathcal{L}_{\text{PDE}}(\theta)$ represents the physics-based constraints from the PDEs, and λ (lambda) parameter allows for tuning the relative importance of these two aspects in training.

6. Conclusions

This review paper has comprehensively explored the evolving field of multiscale modeling in paving materials, highlighting the applications of numerical methods and ML. Through this study, it is evident that multiscale modeling stands as a significant technique in understanding and predicting the behavior of complex civil engineering materials like asphalt mixtures. The hierarchical nature of bituminous mixtures, from the nanoscale to the macroscale, presents unique challenges and opportunities. It is observed that numerical methods provide a robust framework for analyzing and modeling these complexities, enabling engineers to simulate physical phenomena with high accuracy. At the same time, the emergence of ML has opened new avenues, allowing for the incorporation of large datasets and the development of prediction models with higher accuracy and efficiency. The discussion on the integration of numerical methods and ML algorithms underscores a significant advancement in the field. This integration not only enhances the predictive capability of models but also significantly reduces the time and resources required for empirical testing. The ability to accurately predict pavement performance demonstrates the effectiveness of these coupled techniques.

However, the integration of data across different scales, the need for more comprehensive datasets, and the continuous evolution of ML algorithms are areas that require further exploration and development in this field. Additionally, the refinement of numerical simulations and advancements in ML hold the potential to revolutionize the approach to pavement design and maintenance in the future.

In conclusion, this review paper not only sheds light on the current state of multiscale modeling in paving materials but also outlines the path for upcoming research. The integration of numerical simulations and ML marks a substantial progress to create more resilient, economical, and eco-friendly paving alternatives.

CRediT authorship contribution statement

Mahmoud Khadijeh: Writing – review & editing, Writing – original draft, Formal analysis. **Cor Kasbergen:** Supervision, Formal analysis. **Sandra Erkens:** Supervision, Formal analysis. **Aikaterini Varveri:** Writing – review & editing, Supervision, Formal analysis.

Declaration of competing interest

The authors declare that they have no known competing financial interests or personal relationships that could have appeared to influence the work reported in this paper.

Acknowledgment

This publication is part of the project 'A multiscale approach towards future road infrastructure: How to design sustainable paving materials?' (project number 18148) of the research program NWO Talent Programme Veni AES 2020, which is awarded to A.V. and financed by the Dutch Research Council (NWO), Netherlands.

Appendix A. Comparative analysis of FEM and GSCM for asphalt mastic modeling

This appendix presents a comprehensive numerical case study demonstrating the practical application of the techniques discussed in Section 3.2. The study focuses on the identification of Prony series parameters using a Genetic algorithm, followed by the simulation of the DSR test using the Maxwell model. The results are then compared with predictions from the GSCM. The study began with the collection of experimental data from DSR tests, which served as the foundation for subsequent steps. A Genetic algorithm was then applied to identify the Prony series parameters. These parameters were implemented in a FEM to simulate the DSR test, providing predictions of G^*. This study considered fillers as elastic materials, which were combined with the binder to form asphalt mastic. Fig. A.10 illustrates the methodological flow of this case study.

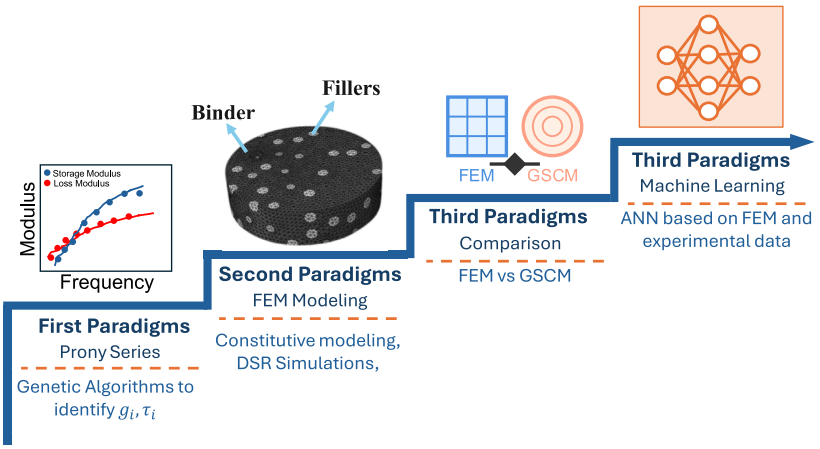

Fig. A.10. Flowchart of the numerical case study, inspired from [137].

The FEM simulation employed several key features to accurately replicate the experimental conditions. An implicit time integration scheme was chosen for the analysis. A logarithmic sweep of frequencies with a range of 0.0159 to 16 Hz was used to replicate the experimental test conditions. Tie contacts were implemented to ensure proper load transfer between different parts of the model. Additionally, a cohesive stiffness contact was defined between the mastic sample and the top and bottom plates (Fig. A.11). The simulation was conducted at a constant temperature of 20 °C to match the experimental conditions.

The Genetic algorithm parameters are chosen to balance thorough exploration of the solution space with computational efficiency. Tables A.7 and A.8 summarizes the key parameters used in this study, including the filler properties, binder properties, Genetic algorithm and Prony series parameters. The results of the numerical simulations are presented in Fig. A.12, which compares the predictions from the FEM model and the GSCM across six different scenarios with varying filler percentages: (a) 28%, (b) 24%,

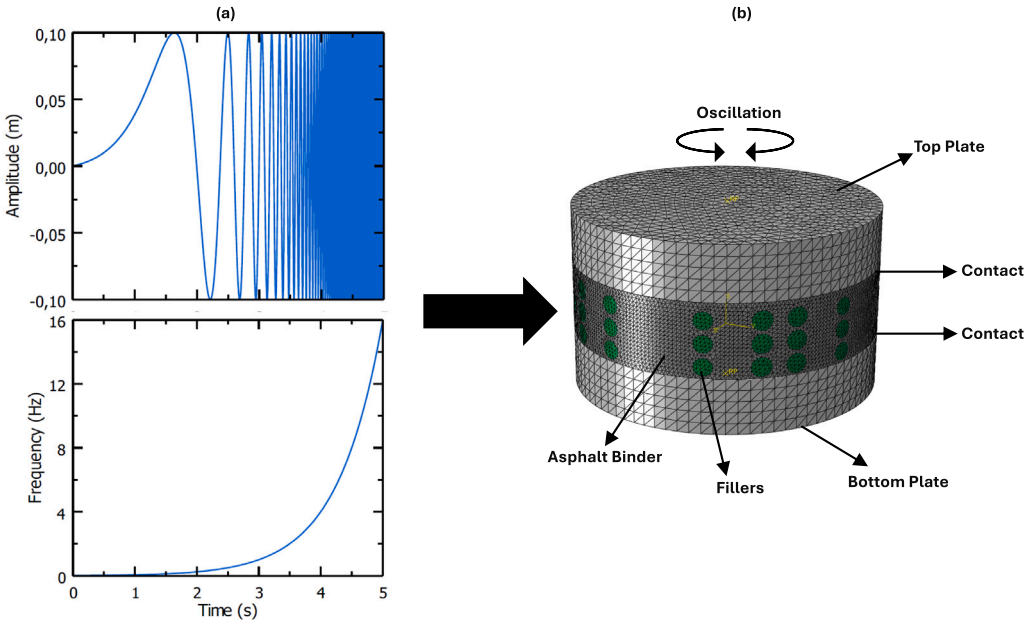

Fig. A.11. FEM setup for DSR testing. (a) Logarithmic sine sweep input: amplitude vs. time (top) and frequency vs. time (bottom). (b) FE model of the DSR test.

Table A.7
Parameters used in the FEM simulation.

Parameter	Value
Temperature [°C]	20 °C
Frequency [Hz]	[0.0159-16]
Population Size	15
Recombination	0.7
Mutation Rate	[0.5, 1]
Number of Prony Parameters	10
Fillers Stiffness [GPa]	70
Fillers [%]	[8-28]
Instantaneous Young's Modulus (E_0) [MPa]	240.5
Poisson's ratio (ν)	0.35

Table A.8
Prony Series Parameters used in the FEM simulation.

i	Relaxation times (τ_i)	Weights (g_i)
1	0.004694686	0.093632628
2	0.115054235	0.117440582
3	0.012508845	0.097836541
4	0.004675019	0.098564454
5	0.033004199	0.093474197
6	0.039371971	0.034233612
7	0.004888031	0.157408419
8	4.005918554	0.051016550
9	0.004949636	0.149722400
10	0.568111227	0.086711249

(c) 20%, (d) 18%, (e) 13%, and (f) 8%. A clear trend emerges across all filler percentages. GSCM consistently predicts higher modulus values than FEM. This difference becomes more pronounced as the filler percentage decreases from 28% to 8%. At higher filler contents, the two methods produce very similar results, but as the filler content reduces, a growing discrepancy appears. Both methods show the characteristic behavior of asphalt materials, with G^* values rising as frequency increases. This indicates that the material becomes stiffer at higher loading rates, which is typical for viscoelastic materials like asphalt mastic.

The divergence between FEM and GSCM predictions at lower filler percentages suggests that these methods may be handling the interaction between the asphalt binder and filler particles differently. GSCM appears to be more sensitive to changes in filler content by overestimating the stiffening effect of the filler at lower concentrations.

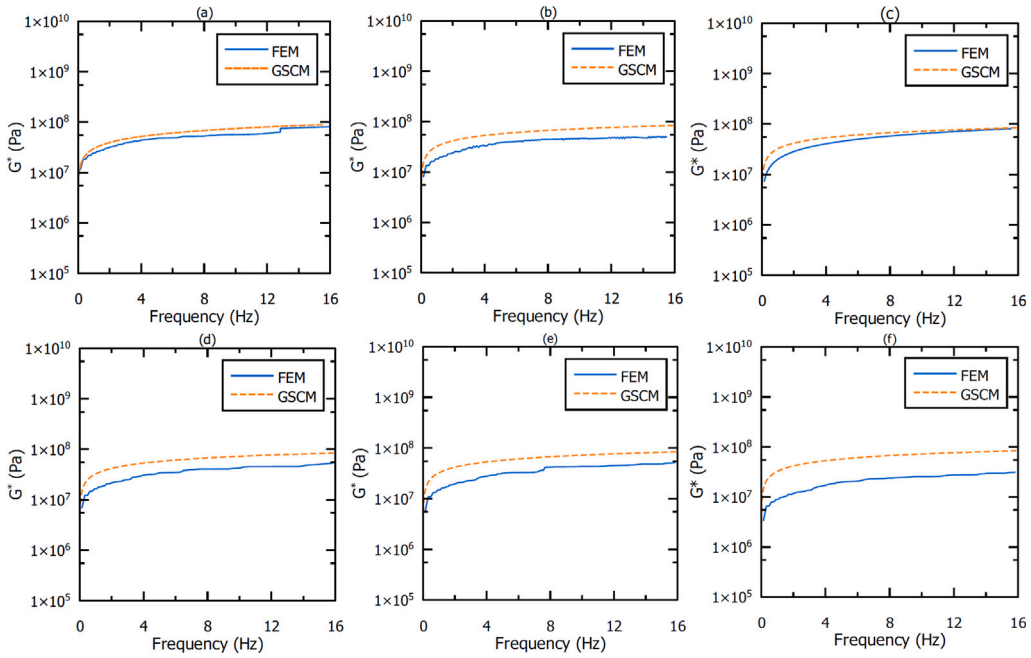

Fig. A.12. Comparison of FEM and GSCM predictions for complex shear modulus (G^*) across different frequencies and filler percentages.

This comparison highlights the need for careful consideration when selecting the modeling method for asphalt mastic, particularly when studying materials with varying filler contents or when precise modulus predictions are required across a range of loading frequencies.

Appendix B. Phase field simulation of microstructural evolution in PMB

This appendix presents a practical example of a PFM applied to study the separation between polymer and bitumen. The simulation demonstrates the evolution of microstructure and phase separation in a PMB system, illustrating the concepts discussed in Section 3.3 of the main text.

The simulation employs a binary PFM based on the Cahn-Hilliard equation. The order parameter $\phi(\mathbf{r}, t)$ represents the local composition, where $\phi = 1$ corresponds to a polymer-rich phase and $\phi = -1$ to a bitumen-rich phase. The free energy functional is given by:

$$F[\phi] = \int_{\Omega} \left[A(\phi^2 - 1)^2 + \frac{\kappa}{2} |\nabla \phi|^2 \right] dV \tag{B.1}$$

where $A(\phi^2-1)^2$ is the bulk free energy density with a double-well potential to encourage phase separation. The gradient term $\frac{\kappa}{2}|\nabla\phi|^2$ penalizes sharp interfaces, leading to a diffuse interface description. The temporal evolution of ϕ is governed by the Cahn-Hilliard equation:

$$\frac{\partial \phi}{\partial t} = M \nabla^2 \left(\frac{\delta F}{\delta \phi} \right) = M \nabla^2 \left(4A\phi(\phi^2 - 1) - \kappa \nabla^2 \phi \right) \tag{B.2}$$

where M is the mobility, assumed constant in this simulation.

The simulation is performed on a 256 × 256 grid using finite difference methods with periodic boundary conditions. Key parameters include a time step of 0.05, double-well potential parameter A of 0.1, gradient energy coefficient κ of 0.1, and mobility M of 1.0. The initial condition is set to mimic a partially mixed state of polymer and bitumen:

$$\phi_0(x, y) = \tanh((0.5 - \sqrt{x^2 + y^2}) \cdot 5) + 0.1 \cdot \text{randn}(x, y) \tag{B.3}$$

This creates a circular polymer-rich domain (positive ϕ) surrounded by a bitumen-rich matrix (negative ϕ), with added random fluctuations to initiate phase separation.

The simulation reveals the evolution of the polymer-bitumen system over time (Fig. B.13). Initially, a rapid breakdown of the circular polymer-rich domain is observed. This is followed by the formation of smaller polymer-rich regions throughout the matrix, and a gradual coarsening of these regions over time. This behavior is consistent with experimental observations in PMB systems, where initial polymer domains disperse and then reorganize within the bitumen matrix. The simulation captures key phenomena

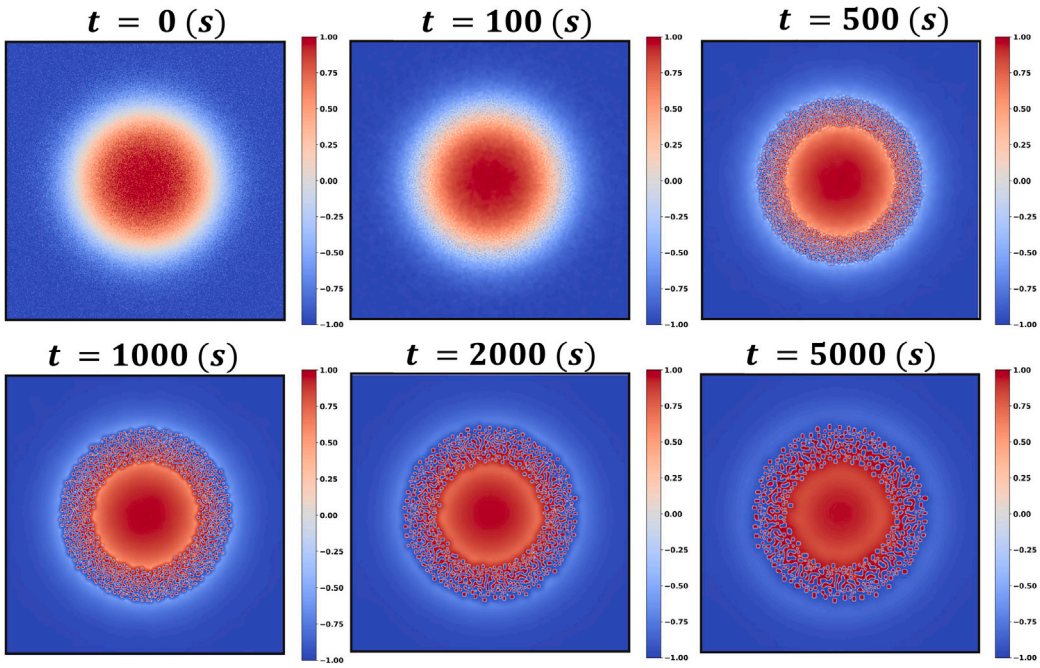

Fig. B.13. Time evolution of phase separation in a polymer-modified bitumen system simulated using the PFM.

such as spinodal decomposition, evidenced by the initial rapid formation of polymer-rich and bitumen-rich regions. Additionally, larger polymer-rich areas grow while smaller ones shrink and disappear, a process known as Ostwald ripening.

Additionally, the simulation demonstrates interface dynamics, maintaining diffuse interfaces between phases, which is characteristic of the phase-field approach. The evolution of the system provides insights into the microstructural development of PMB materials. The final distribution and size of polymer-rich domains can significantly influence the mechanical and rheological properties of the mixture.

This simulation example demonstrates the capability of PFM to model complex microstructural evolution in bituminous mixtures. By adjusting parameters such as A, κ, and M, various scenarios relevant to PMB systems can be explored. These include different polymer concentrations (by modifying the initial condition), varying interaction strengths between polymer and bitumen (by adjusting A), and different processing conditions (through changes in M and κ). Such simulations can guide the optimization of PMB formulations and processing conditions to achieve desired microstructures and, consequently, enhanced material properties.

However, this model represents a simplified binary system, whereas real bitumen is a complex mixture of many components. Additionally, the model does not account for temperature-dependent behavior, which is crucial in bitumen systems. Furthermore, mechanical properties and their coupling with phase separation are not included in this simulation. Future work could address these limitations by extending to multi-component systems to include SARA fractions, incorporating temperature-dependent parameters, and coupling with mechanical models to simulate the interplay between microstructure and material properties.

Data availability

No data was used for the research described in the article.

References

[1] S. Lync, Multiscale modeling techniques in CAE | skill-lync | workshop, 2021.
[2] S. Kim, H. Shin, Deep learning framework for multiscale finite element analysis based on data-driven mechanics and data augmentation, Comput. Methods Appl. Mech. Engrg. 414 (2023) http://dx.doi.org/10.1016/j.cma.2023.116131.
[3] N. Kevlahan, Principles of multiscale modeling, Phys. Today 65 (2012) 56, http://dx.doi.org/10.1063/PT.3.1609.
[4] M. Yin, E. Zhang, Y. Yu, G. Karniadakis, Interfacing finite elements with deep neural operators for fast multiscale modeling of mechanics problems, Comput. Methods Appl. Mech. Engrg. 402 (2022) http://dx.doi.org/10.1016/j.cma.2022.115027.
[5] G. Sherzer, P. Gao, E. Schlangen, G. Ye, E. Gal, Upscaling cement paste microstructure to obtain the fracture, shear, and elastic concrete mechanical LDPM parameters, Materials 10 (2017) http://dx.doi.org/10.3390/ma10030242.
[6] K. Karapiperis, L. Stainier, M. Ortiz, J. Andrade, Data-driven multiscale modeling in mechanics, J. Mech. Phys. Solids 147 (2021) 104–239, http://dx.doi.org/10.1016/j.jmps.2020.104239.

[7] C.E. Sawda, F. Fakhari-Tehrani, J. Absi, F. Allou, C. Petit, Multiscale heterogeneous numerical simulation of asphalt mixture, Mater. Des. Process. Commun. 1 (2019) 1–7, http://dx.doi.org/10.1002/mdp2.42.
[8] A. Sakhaee-Pour, W. Li, Two-scale geomechanics of shale, SPE Reserv. Eval. Eng. (2018) 1–12, http://dx.doi.org/10.2118/189965-pa.
[9] W. Huang, Z. Ren, X. Zhang, J. Yu, Investigation on microstructural damage properties of asphalt mixture using linear and damage-coupled viscoelastic model, Appl. Sci. (2019) http://dx.doi.org/10.3390/app9020303.
[10] R. Jing, A. Varveri, X. Liu, A. Scarpas, S. Erkens, Laboratory and field aging effect on bitumen chemistry and rheology in porous asphalt mixture, Transp. Res. Rec. 2673 (2019) 365–374, http://dx.doi.org/10.1177/0361198119833362.
[11] F. Tao, X. Liu, H. Du, W. Yu, Finite element coupled positive definite deep neural networks mechanics system for constitutive modeling of composites, Comput. Methods Appl. Mech. Engrg. 391 (2022) http://dx.doi.org/10.1016/j.cma.2021.114548.
[12] X. Yu, N. Burnham, M. Tao, Surface microstructure of bitumen characterized by atomic force microscopy surface microstructure of bitumen characterized by atomic force microscopy, Adv. Colloid Interface Sci. 218 (2015) 17–33, http://dx.doi.org/10.1016/j.cis.2015.01.003.
[13] P. Redelius, The structure of asphaltenes in bitumen, Road Mater. Pavement Des. 7 (2006) 143–162, http://dx.doi.org/10.1080/14680629.2006.9690062.
[14] E. Omairey, F. Gu, Y. Zhang, An equation-based multiphysics modelling framework for oxidative ageing of asphalt pavements, J. Clean. Prod. 280 (2021) 124401, http://dx.doi.org/10.1016/j.jclepro.2020.124401.
[15] D. Lesueur, Evidence of the colloidal structure of bitumen, in: ISAP International Workshop on Chemo-Mechanics of Bituminous Materials, 2009, pp. 39–48.
[16] X. Zhang, I. Hoff, Comparative study of thermal-oxidative aging and salt solution aging on bitumen performance, Materials (2021) http://dx.doi.org/10.3390/ma14051174.
[17] G. E., J. Zhang, Q. Shen, P. Ji, J. Wang, Y. Xiao, Influence of filler type and rheological properties of asphalt mastic on the asphalt mastic–aggregate interaction, Materials 16 (2023) http://dx.doi.org/10.3390/ma16020574.
[18] F. Mastoras, A. Varveri, M. van Tooren, S. Erkens, Effect of mineral fillers on ageing of bituminous mastics, Constr. Build. Mater. 276 (2021) 122215, http://dx.doi.org/10.1016/j.conbuildmat.2020.122215.
[19] B. Xing, C. Fang, X. Lyu, W. Fan, Y. Lyu, Influence of mineral filler characteristics on the filler–asphalt interfacial behavior, Adv. Powder Technol. 35 (10) (2024) 104636, http://dx.doi.org/10.1016/j.apt.2024.104636.
[20] A. Akbari, A. Akbari, A. Ghanbari, S. Hesami, Investigating the influence of aging and filler type on the fatigue behavior of bitumen mastics, Constr. Build. Mater. 269 (2021) 121254, http://dx.doi.org/10.1016/j.conbuildmat.2020.121254.
[21] N. Mukhtar, M.M. Hasan, M.M. Ghazali, Z.M. Zin, K. Shariff, A. Sani, Influence of concentration and packing of filler particles on the stiffening effect and shearing behaviour of asphalt mastic, Constr. Build. Mater. 295 (2021) 123660, http://dx.doi.org/10.1016/j.conbuildmat.2021.123660.
[22] A. Al-Mohammedawi, K. Mollenhauer, A study on the influence of the chemical nature of fillers on rheological and fatigue behavior of bitumen emulsion mastic, Materials 13 (2020) 1–22, http://dx.doi.org/10.3390/ma13204627.
[23] K. Zhang, G. Wei, W. Xie, B. Yang, W. Li, Y. Luo, A novel evaluation method of construction homogeneity for asphalt pavement based on the characteristic of component distribution, Materials 15 (2022) http://dx.doi.org/10.3390/ma15207284.
[24] P. Cui, Y. Xiao, B. Yan, M. Li, S. Wu, Morphological characteristics of aggregates and their influence on the performance of asphalt mixture, Constr. Build. Mater. 186 (2018) 303–312, http://dx.doi.org/10.1016/j.conbuildmat.2018.07.124.
[25] J. Zheng, T. Huang, Study on triaxial test method and failure criterion of asphalt mixture, J. Traffic Transp. Eng. 2 (2015) 93–106, http://dx.doi.org/10.1016/j.jtte.2015.02.003.
[26] A. Gundla, Use of Micro-Mechanical Models to Study the Mastic Level Structure of Asphalt Concretes Containing Reclaimed Asphalt Pavement (Ph.D. thesis), Arizona State University, 2014.
[27] H. Li, X. Luo, F. Ma, Y. Zhang, Micromechanics modeling of viscoelastic asphalt-filler composite system with and without fatigue cracks, Mater. Des. 209 (2021) http://dx.doi.org/10.1016/j.matdes.2021.109983.
[28] F. Aragao, Computational Microstructure Modeling of Asphalt Mixtures Subjected to Rate-Dependent Fracture (Ph.D. thesis), University of Nebraska - Lincoln, 2011.
[29] J. Chen, H. Dan, Y. Ding, Y. Gao, M. Guo, S. Guo, B. Han, B. Hong, Y. Hou, C. Hu, J. Hu, J. Huyan, J. Jiang, W. Jiang, C. Li, P. Liu, Y. Liu, Z. Liu, G. Lu, J. Ouyang, X. Qu, D. Ren, C. Wang, C. Wang, D. Wang, D. Wang, H. Wang, H. Wang, Y. Xiao, C. Xing, H. Xu, Y. Yan, X. Yang, L. You, Z. You, B. Yu, H. Yu, H. Yu, H. Zhang, J. Zhang, C. Zhou, C. Zhou, X. Zhu, New innovations in pavement materials and engineering: A review on pavement engineering research 2021, J. Traffic Transp. Eng. 8 (2021) 815–999, http://dx.doi.org/10.1016/j.jtte.2021.10.001.
[30] H. Wang, X. Liu, H. Zhang, P. Apostolidis, S. Erkens, A. Skarpas, Micromechanical modelling of complex shear modulus of crumb rubber modified bitumen, Mater. Des. 188 (2020) 108467, http://dx.doi.org/10.1016/j.matdes.2019.108467.
[31] C. Pichler, R. Lackner, E. Aigner, Generalized self-consistent scheme for upscaling of viscoelastic properties of highly-filled matrix-inclusion composites - Application in the context of multiscale modeling of bituminous mixtures, Composites B 43 (2012) 457–464, http://dx.doi.org/10.1016/j.compositesb.2011.05.034.
[32] N. Kovachki, B. Liu, X. Sun, H. Zhou, K. Bhattacharya, M. Ortiz, A. Stuart, Multiscale modeling of materials: Computing, data science, uncertainty and goal-oriented optimization, Mech. Mater. 165 (2022) 104156, http://dx.doi.org/10.1016/j.mechmat.2021.104156.
[33] M. Smith, ABAQUS/Standard User's Manual, Version 6.9, Dassault Systèmes Simulia Corp, United States, 2009.
[34] M. Björklund, K. Larsson, M. Larson, Error estimates for finite element approximations of viscoelastic dynamics: The generalized Maxwell model, Comput. Methods Appl. Mech. Engrg. 425 (2024) http://dx.doi.org/10.1016/j.cma.2024.116933.
[35] A. Shukla, Y.M. Joshi, Boltzmann superposition principle for a time-dependent soft material: assessment under creep flow field, Rheol. Acta 56 (2017) 927–940, http://dx.doi.org/10.1007/s00397-017-1044-x.
[36] J.C. Simo, T.J. Hughes, Computational Inelasticity, vol. 7, Springer Science & Business Media, 2006, http://dx.doi.org/10.1007/b98904.
[37] D. Netzband, DMA2PRONY _ OPT. Online MATLAB Tool.
[38] R. Luo, H. Lv, H. Liu, Development of prony series models based on continuous relaxation spectrums for relaxation moduli determined using creep tests, Constr. Build. Mater. 168 (2018) 758–770, http://dx.doi.org/10.1016/j.conbuildmat.2018.02.036.
[39] M. Khadijeh, A. Varveri, C. Kasbergen, S. Erkens, Prony series fit for viscoelastic data using a genetic algorithm, 2024, http://dx.doi.org/10.5281/zenodo.13735908.
[40] M. Ramzanpour, M. Hosseini-Farid, M. Ziejewski, G. Karami, A constrained particle swarm optimization algorithm for hyperelastic and visco-hyperelastic characterization of soft biological tissues, Int. J. Comput. Methods Eng. Sci. Mech. 21 (4) (2020) 169–184, http://dx.doi.org/10.1080/15502287.2020.1767725.
[41] J. Kennedy, R. Eberhart, Particle swarm optimization, in: Proceedings of ICNN'95-International Conference on Neural Networks, Vol. 4, IEEE, 1995, pp. 1942–1948, http://dx.doi.org/10.1109/ICNN.1995.488968.
[42] J.C. Mauro, Y.Z. Mauro, On the prony series representation of stretched exponential relaxation, Physica A 506 (2018) 75–87, http://dx.doi.org/10.1016/j.physa.2018.04.047.
[43] G. Dondi, V. Vignali, M. Pettinari, F. Mazzotta, A. Simone, C. Sangiorgi, Modeling the DSR complex shear modulus of asphalt binder using 3D discrete element approach, Constr. Build. Mater. 54 (2014) 236–246, http://dx.doi.org/10.1016/j.conbuildmat.2013.12.005.
[44] S. Somé, V. Gaudefroy, A. Pavoine, Viscoelastic behavior of fluxed asphalt binders and mixes, in: 22ème Congrès Français de Mécanique, 215.

[45] J. Londono, L. Berger-Vergiat, H. Waisman, An equivalent stress-gradient regularization model for coupled damage-viscoelasticity, Comput. Methods Appl. Mech. Engrg. 322 (2017) 137–166, http://dx.doi.org/10.1016/j.cma.2017.04.010.
[46] J. Wu, V. Nguyen, C. Nguyen, D. Sutula, S. Sinaie, Phase-field modelling of fracture, Adv. Appl. Mech. 53 (2020) 1–183, http://dx.doi.org/10.1016/bs.aams.2019.08.001.
[47] S. Zhou, X. Zhuang, T. Rabczuk, Phase field modeling of brittle compressive-shear fractures in rock-like materials: A new driving force and a hybrid formulation, Comput. Methods Appl. Mech. Engrg. 355 (2019) 729–752, http://dx.doi.org/10.1016/j.cma.2019.06.021.
[48] L. Chen, Phase-field models for microstructure evolution, Annu. Rev. Mater. Sci. 32 (2002) 113–140, http://dx.doi.org/10.1146/annurev.matsci.32.112001.132041.
[49] A. Novick-Cohen, L.A. Segel, Nonlinear aspects of the Cahn–Hilliard equation, Physica D 10 (3) (1984) 277–298, http://dx.doi.org/10.1016/0167-2789(84)90180-5.
[50] J. Zhu, X. Lu, R. Balieu, N. Kringos, Modelling and numerical simulation of phase separation in polymer modified bitumen by phase-field method, Mater. Des. 107 (2016) 322–332, http://dx.doi.org/10.1016/j.matdes.2016.06.041.
[51] M. Liang, X. Xin, W. Fan, H. Wang, W. Sun, Phase field simulation and microscopic observation of phase separation and thermal stability of polymer modified asphalt, Constr. Build. Mater. 204 (2019) 132–143, http://dx.doi.org/10.1016/j.conbuildmat.2019.01.180.
[52] Y. Hou, L. Wang, P. Yue, T. Pauli, W. Sun, Modeling mode I cracking failure in asphalt binder by using nonconserved phase-field model, J. Mater. Civ. Eng 26 (4) (2014) 684–691, http://dx.doi.org/10.1061/(ASCE)MT.1943-5533.0000874.
[53] F. Rosenblatt, The perceptron: A probabilistic model for information storage and organization in the brain, Psychol. Rev. 65 (1958) 386–408, http://dx.doi.org/10.1037/h0042519.
[54] O.M. López, A.M. López, J. Crossa, Multivariate statistical machine learning methods for genomic prediction, 2022, http://dx.doi.org/10.1007/978-3-030-89010-0.
[55] N. Babu, A. Aravind, A. Rakesh, M. Jahzan, R. Prabha, M.R. Viswanathan, Automatic fault classification for journal bearings using ANN and DNN, Arch. Acoust. 43 (2018) 727–738, http://dx.doi.org/10.24425/aoa.2018.125166.
[56] A. Malik, A. Kumar, P. Rai, A. Kuriqi, Prediction of multi-scalar standardized precipitation index by using artificial intelligence and regression models, Climate 9 (2021) 1–25, http://dx.doi.org/10.3390/cli9020028.
[57] T. Ghalandari, L. Shi, F. Sadeghi-Khanegah, W.V. den bergh, C. Vuye, Utilizing artificial neural networks to predict the asphalt pavement profile temperature in western Europe, Case Stud. Constr. Mater. 18 (2023) http://dx.doi.org/10.1016/j.cscm.2023.e02130.
[58] L. Wu, V. Nguyen, N. Kilingar, L. Noels, A recurrent neural network-accelerated multi-scale model for elasto-plastic heterogeneous materials subjected to random cyclic and non-proportional loading paths, Comput. Methods Appl. Mech. Engrg. 369 (2020) http://dx.doi.org/10.1016/j.cma.2020.113234.
[59] L. Alzubaidi, J. Zhang, A. Humaidi, A. Al-Dujaili, Y. Duan, O. Al-Shamma, J. Santamaría, M. Fadhel, M. Al-Amidie, L. Farhan, Review of deep learning: concepts, CNN architectures, challenges, applications, future directions, J. Big Data (2021) http://dx.doi.org/10.1186/s40537-021-00444-8.
[60] C. Zhang, E. Nateghinia, L. Miranda-Moreno, L. Sun, Pavement distress detection using convolutional neural network (CNN): A case study in Montreal, Canada, Int. J. Transp. Sci. Technol. 11 (2022) 298–309, http://dx.doi.org/10.1016/j.ijtst.2021.04.008.
[61] J. Schmidhuber, Deep learning in neural networks: An overview, J. Neural Netw. 61 (2015) 85–117, http://dx.doi.org/10.1016/j.neunet.2014.09.003.
[62] P.H. Thike, Z. Zhao, P. Shi, Y. Jin, Significance of artificial neural network analytical models in materials' performance prediction, Bull. Mater. Sci. B 43 (2020) http://dx.doi.org/10.1007/s12034-020-02154-y.
[63] U. Paturi, S. Cheruku, N. Reddy, The role of artificial neural networks in prediction of mechanical and tribological properties of composites—A comprehensive review, Arch. Comput. (2022) http://dx.doi.org/10.1007/s11831-021-09691-7.
[64] M. Kraus, M. Schuster, J. Kuntsche, G. Siebert, J. Schneider, Parameter identification methods for visco- and hyperelastic material models, Glass Struct. Eng. 2 (2017) 147–167, http://dx.doi.org/10.1007/s40940-017-0042-9.
[65] V. Vignali, F. Mazzotta, C. Sangiorgi, A. Simone, C. Lantieri, G. Dondi, Rheological and 3D DEM characterization of potential rutting of cold bituminous mastics, Constr. Build. Mater. 73 (2014) 339–349, http://dx.doi.org/10.1016/j.conbuildmat.2014.09.051.
[66] H. Fadil, D. Jelagin, M. Partl, A new viscoelastic micromechanical model for bitumen-filler mastic, Constr. Build. Mater. 253 (2020) 119062, http://dx.doi.org/10.1016/j.conbuildmat.2020.119062.
[67] A. Bhasin, V. Ganesan, Preliminary investigation of using a multi-component phase field model to evaluate microstructure of asphalt binders, Int. J. Pavement Eng. 18 (2017) 775–782, http://dx.doi.org/10.1080/10298436.2015.1065998.
[68] A. Lyne, V. Wallqvist, M. Rutland, P. Claesson, B. Birgisson, Surface wrinkling: The phenomenon causing bees in bitumen, J. Mater. Sci. 48 (2013) 6970–6976, http://dx.doi.org/10.1007/s10853-013-7505-4.
[69] Y. Hu, M. Allanson, A. Sreeram, J. Ryan, H. Wang, L. Zhou, B. Hofko, G.D. Airey, Characterisation of bitumen through multiple ageing-rejuvenation cycles, Int. J. Pavement Eng. 25 (1) (2024) 2365350, http://dx.doi.org/10.1080/10298436.2024.2365350.
[70] Y. Hu, W. Si, X. Kang, Y. Xue, H. Wang, T. Parry, G.D. Airey, State of the art: Multiscale evaluation of bitumen ageing behaviour, Fuel 326 (2022) 125045, http://dx.doi.org/10.1016/j.fuel.2022.125045.
[71] M. Porto, R. Angelico, P. Caputo, A. Abe, B. Teltayev, C. Rossi, The structure of bitumen: Conceptual models and experimental evidences, Materials 15 (2022) http://dx.doi.org/10.3390/ma15030905.
[72] T. Wang, J. Wang, X. Hou, F. Xiao, Effects of SARA fractions on low temperature properties of asphalt binders, Road Mater. Pavement Des. 22 (2021) 539–556, http://dx.doi.org/10.1080/14680629.2019.1628803.
[73] J. Wang, T. Wang, X. Hou, F. Xiao, Modelling of rheological and chemical properties of asphalt binder considering SARA fraction, Fuel 238 (2019) 320–330, http://dx.doi.org/10.1016/j.fuel.2018.10.126.
[74] T. Meier, G. Dresen, M. Makasi, A. Reinicke, E. Rybacki, What controls the mechanical properties of shale rocks? – Part I: Strength and Young's modulus, J. Pet. Sci. Eng. 135 (2015) 702–722, http://dx.doi.org/10.1016/j.petrol.2015.10.028.
[75] W. Li, A. Sakhaee-Pour, Two-scale geomechanics of carbonates, Rock Mech. Rock Eng. 51 (2018) 3667–3679, http://dx.doi.org/10.1007/s00603-018-1536-8.
[76] P. Apostolidis, C. Kasbergen, A. Bhasin, A. Scarpas, S. Erkens, Study of asphalt binder fatigue with a new dynamic shear rheometer geometry, Transp. Res. Rec. 2672 (2018) 290–300, http://dx.doi.org/10.1177/0361198118781378.
[77] E. Ziade, F.F. Tehrani, A. Beghin, C. Petit, J. Absi, A. Millien, P. Reynaud, Experimental and numerical investigation on the rheological behaviour of bituminous composites via DSR testing, Road Mater. Pavement Des. 22 (2021) S328–S344, http://dx.doi.org/10.1080/14680629.2021.1912812.
[78] G. Câmara, R. Micaelo, N.M. Azevedo, 3D DEM model simulation of asphalt mastics with sunflower oil, Computer (2023) http://dx.doi.org/10.1007/s40571-023-00574-1.
[79] J. Zhu, R. Balieu, X. Lu, N. Kringos, Numerical investigation on phase separation in polymer-modified bitumen: effect of thermal condition, J. Mater. Sci. 52 (2017) 6525–6541, http://dx.doi.org/10.1007/s10853-017-0887-y.
[80] Y. Hou, L. Wang, P. Yue, W. Sun, Fracture failure in crack interaction of asphalt binder by using a phase field approach, Mater. Struct. 48 (2015) 2997–3008, http://dx.doi.org/10.1617/s11527-014-0372-x.
[81] X. Ma, X. Zhang, J. Hou, S. Song, H. Chen, D. Kuang, Predicting dynamic properties of asphalt mastic considering asphalt-filler interaction based on 2S2P1D model, Materials 15 (2022) http://dx.doi.org/10.3390/ma15165688.

[82] X. Yang, J. Guan, L. Ding, Z. You, V. Lee, M.M. Hasan, X. Cheng, Research and applications of artificial neural network in pavement engineering: A state-of-the-art review, J. Traffic Transp. Eng. 8 (2021) 1000–1021, http://dx.doi.org/10.1016/j.jtte.2021.03.005.
[83] J. Useche-Castelblanco, O. Reyes-Ortiz, A. Alvarez, Application of machine learning models for prediction of rheological properties of wax-modified asphalt binders, Constr. Build. Mater. 395 (2023) http://dx.doi.org/10.1016/j.conbuildmat.2023.132352.
[84] A. Hamid, H. Baaj, M. El-Hakim, Predicting the recovery and nonrecoverable compliance behaviour of asphalt binders using artificial neural networks, Processes 10 (2022) 1–20, http://dx.doi.org/10.3390/pr10122633.
[85] M. Alas, S. Ali, Prediction of the high-temperature performance of a geopolymer modified asphalt binder using artificial neural networks, Int. J. Technol. 10 (2019) 417–427, http://dx.doi.org/10.14716/ijtech.v10i2.2421.
[86] K. Yan, L. You, Investigation of complex modulus of asphalt mastic by artificial neural networks, Indian J. Eng. Mater. 21 (2014) 445–450.
[87] V. Venudharan, K. Biligiri, Heuristic principles to predict the effect of crumb rubber gradation on asphalt binder rutting performance, J Mater. Civ. Eng. 29 (2017) 1–10, http://dx.doi.org/10.1061/(asce)mt.1943-5533.0001880.
[88] R. Botella, D.L. Presti, K. Vasconcelos, K. Bernatowicz, A. Martínez, R. Miró, L. Specht, E. Mercado, G. Pires, E. Pasquini, C. Ogbo, F. Preti, M. Pasetto, A. del Barco Carrión, A. Roberto, M. Orešković, K. Kuna, G. Guduru, A. Martin, A. Carter, G. Giancontieri, A. Abed, E. Dave, G. Tebaldi, Machine learning techniques to estimate the degree of binder activity of reclaimed asphalt pavement, Mater. Struct. 55 (2022) http://dx.doi.org/10.1617/s11527-022-01933-9.
[89] K. Zhong, Q. Meng, M. Sun, G. Luo, Artificial neural network (ANN) modeling for predicting performance of SBS modified asphalt, Materials 15 (2022) http://dx.doi.org/10.3390/ma15238695.
[90] H. Yao, M. Xu, J. Liu, Y. Liu, J. Ji, Z. You, Literature review on the discrete element method in asphalt mixtures, Fmats 9 (2022) http://dx.doi.org/10.3389/fmats.2022.879245.
[91] D. Wang, X. Ding, L. Gu, T. Ma, Assessment model and virtual simulation for fatigue damage evolution of asphalt mortar and mixture, Adv. Mater. Sci. Eng. (2018) http://dx.doi.org/10.1155/2018/5904807.
[92] L. Gao, H. Kong, X. Deng, Z. Wang, Multi-scale finite element simulation of asphalt mixture anti-cracking performance, Theor. Appl. Fract. Mech. 121 (2022) 103490, http://dx.doi.org/10.1016/j.tafmec.2022.103490.
[93] L. Ruan, R. Luo, D. Zhang, B. Wang, Numerical simulation of crack paths in asphalt mixture using ordinary state-based peridynamics, Mater. Struct. 54 (2021) 1–19, http://dx.doi.org/10.1617/s11527-021-01685-y.
[94] W. Huang, H. Wang, Y. Yin, X. Zhang, J. Yuan, Microstructural modeling of rheological mechanical response for asphalt mixture using an image-based, Materials (2019) http://dx.doi.org/10.3390/ma12132041.
[95] M. Gajewski, J. Król, The influence of mortar's Poisson ratio and viscous properties on effective stiffness and anisotropy of asphalt mixture, Materials 15 (2022) http://dx.doi.org/10.3390/ma15248946.
[96] I. Menapace, W. Yiming, E. Masad, Effects of environmental factors on the chemical composition of asphalt binders, Energy Fuels 33 (4) (2018) 2614–2624, http://dx.doi.org/10.1021/acs.energyfuels.8b03273.
[97] L. He, M. Chen, Y. Tan, Z. Zhao, Y. Hu, M. Zhao, Evaluation of the viscoelastic characteristic of asphalt binder with dry–wet cycle aging, J. Mater. Civ. Eng. 36 (6) (2024) 04024119, http://dx.doi.org/10.1061/JMCEE7.MTENG-17313.
[98] E. Mączka, P. Mackiewicz, Asphalt mixtures and flexible pavement construction degradation considering different environmental factors, Appl. Sci. 12 (23) (2022) http://dx.doi.org/10.3390/app122312068.
[99] Y. Zhao, J. Jiang, Y. Dai, L. Zhou, F. Ni, Thermal property evaluation of porous asphalt concrete based on heterogeneous meso-structure finite element simulation, Appl. Sci. 10 (2020) http://dx.doi.org/10.3390/app10051671.
[100] P. Liu, C. Du, J. Friederichs, Y. Wang, J. Hu, S. Leischner, Multiscale modelling and simulation for asphalt pavements under moving tire footprint loads, Int. J. Pavement Eng. 24 (2023) http://dx.doi.org/10.1080/10298436.2022.2154349.
[101] M. Maia, I. Rocha, P. Kerfriden, F. van der Meer, Physically recurrent neural networks for path-dependent heterogeneous materials: embedding constitutive models in a data-driven surrogate, Comput. Methods Appl. Mech. Engrg. (2022) http://dx.doi.org/10.1016/j.cma.2023.115934.
[102] P. Das, H. Baaj, N. Kringos, S. Tighe, Coupling of oxidative ageing and moisture damage in asphalt mixtures, Road Mater. Pavement Des. 16 (2015) 265–279, http://dx.doi.org/10.1080/14680629.2015.1030835.
[103] M. Shakiba, M. Darabi, R.A. Al-Rub, E. Masad, D. Little, Microstructural modeling of asphalt concrete using a coupled moisture-mechanical constitutive relationship, Int. J. Solids Struct. 51 (2014) 4260–4279, http://dx.doi.org/10.1016/j.ijsolstr.2014.08.012.
[104] S. Caro, E. Masad, A. Bhasin, D. Little, Coupled micromechanical model of moisture-induced damage in asphalt mixtures, J. Mater. Civ. Eng. 22 (2010) 380–388, http://dx.doi.org/10.1061/(asce)mt.1943-5533.0000031.
[105] M. Nobakht, Characterization of Coupled Aging-Moisture Degradation for Hot Mix Asphalt Concrete (Ph.D. thesis), Texas A&M University, 2018.
[106] L.A. Khateeb, K. Anupam, S. Erkens, T. Scarpas, Micromechanical simulation of porous asphalt mixture compaction using discrete element method (DEM), Constr. Build. Mater. 301 (2021) http://dx.doi.org/10.1016/j.conbuildmat.2021.124305.
[107] D. Zhang, L. Gu, J. Zhu, Effects of aggregate mesostructure on permanent deformation of asphalt mixture using three-dimensional discrete element modeling, Materials 12 (2019) http://dx.doi.org/10.3390/ma12213601.
[108] Q. Dai, Z. You, Micromechanical finite element framework for predicting viscoelastic properties of asphalt mixtures, Mater. Struct. 41 (2008) 1025–1037, http://dx.doi.org/10.1617/s11527-007-9303-4.
[109] X. Zhu, H. Yu, G. Qian, D. Yao, W. Dai, H. Zhang, J. Li, H. Zhong, Evaluation of asphalt mixture micromechanical behavior evolution in the failure process based on discrete element method, Case Stud. Constr. Mater. 18 (2023) http://dx.doi.org/10.1016/j.cscm.2022.e01773.
[110] Y. Yuan, X. Zhu, L. Li, H. Wang, Effect of the interfacial zone on the tensile-damage behavior of an asphalt mixture containing MSWI bottom ash aggregates, J. Mater. Civ. Eng. 29 (2017) http://dx.doi.org/10.1061/(asce)mt.1943-5533.0001792.
[111] G. Câmara, N. Azevedo, R. Micaelo, Impact of rejuvenator-modified mastic on asphalt mixture stiffness: Meso-scale discrete element method approach, Buildings 13 (2023) http://dx.doi.org/10.3390/buildings13123023.
[112] S. Chen, L. Xu, S. Jia, J. Wang, Characterization of the nonlinear viscoelastic constitutive model of asphalt mixture, Case Stud. Constr. Mater. 18 (2023) 1–11, http://dx.doi.org/10.1016/j.cscm.2023.e01902.
[113] Y. Zhang, X. Liu, B. Yin, W. Luo, A nonlinear fractional viscoelastic-plastic creep model of asphalt mixture, Polymers 13 (2021) 1–11, http://dx.doi.org/10.3390/polym13081278.
[114] A. Seitllari, Y. Kumbargeri, K. Biligiri, I. Boz, A soft computing approach to predict and evaluate asphalt mixture aging characteristics using asphaltene as a performance indicator, Mater. Struct. 5 (2019) http://dx.doi.org/10.1617/s11527-019-1402-5.
[115] G. Moussa, M. Owais, Pre-trained deep learning for hot-mix asphalt dynamic modulus prediction with laboratory effort reduction, Constr. Build. Mater. 265 (2020) 120239, http://dx.doi.org/10.1016/j.conbuildmat.2020.120239.
[116] S. El-Badawy, R.A. El-Hakim, A. Awed, Comparing artificial neural networks with regression models for hot-mix asphalt dynamic modulus prediction, J. Mater. Civ. Eng 30 (2018) 1–11, http://dx.doi.org/10.1061/(asce)mt.1943-5533.0002282.
[117] A. Haddad, G. Chehab, G. Saad, The use of deep neural networks for developing generic pavement rutting predictive models models, Int. J. Pavement Eng. (2021) 1–17, http://dx.doi.org/10.1080/10298436.2021.1942466.
[118] T. Le, H. Nguyen, B. Pham, M. Nguyen, C. Pham, N. Nguyen, T. Le, H. Ly, Artificial intelligence-based model for the prediction of dynamic modulus of stone mastic asphalt, Appl. Sci. 10 (2020) http://dx.doi.org/10.3390/APP10155242.

[119] D.R. Eidgahee, H. Jahangir, N. Solatifar, P. Fakharian, M. Rezaeemanesh, Data-driven estimation models of asphalt mixtures dynamic modulus using ANN, GP and combinatorial GMDH approaches, Neural Comput. Appl. 34 (2022) 17289–17314, http://dx.doi.org/10.1007/s00521-022-07382-3.
[120] K. Othman, Artificial neural network models for the estimation of the optimum asphalt content of asphalt mixtures, Int. J. Pavement Res. Technol. 16 (2023) 1059–1071, http://dx.doi.org/10.1007/s42947-022-00179-6.
[121] O. Kaya, Development of neural network-based asphalt mix design parameters prediction tool, Adv. Mater. Sci. Eng. 48 (2023) 12793–12804, http://dx.doi.org/10.1007/s13369-022-07579-7.
[122] F. Xiao, S. Amirkhanian, M. Asce, C. Juang, F. Asce, Prediction of fatigue life of rubberized asphalt concrete mixtures containing reclaimed asphalt pavement using artificial neural networks, J. Mater. Civ. Eng. 21 (2019) http://dx.doi.org/10.1061/(ASCE)0899-1561(2009)21:6(253).
[123] J. Rivera-Pérez, I. Al-Qadi, Asphalt concrete mix design optimization using autoencoder deep neural networks, Transp. Res. Rec. 2678 (2024) 426–438, http://dx.doi.org/10.1177/03611981231171153.
[124] M. Alber, A.B. Tepole, W. Cannon, S. De, S. Dura-Bernal, K. Garikipati, G. Karniadakis, W. Lytton, P. Perdikaris, L. Petzold, E. Kuhl, Integrating machine learning and multiscale modeling—perspectives, challenges, and opportunities in the biological, biomedical, and behavioral sciences, NPJ Digit. Med. 2 (2019) http://dx.doi.org/10.1038/s41746-019-0193-y.
[125] B. Underwood, Multiscale Modeling Approach for Asphalt Concrete and its Implications on Oxidative Aging, Elsevier Ltd., 2015, http://dx.doi.org/10.1016/B978-0-08-100269-8.00009-X.
[126] R. Yousif, S. Tayh, I. Al-Saadi, A. Jasim, Physical and rheological properties of asphalt binder modified with recycled fibers, Adv. Civ. Eng. 2022 (2022) http://dx.doi.org/10.1155/2022/1223467.
[127] M. Anjum, K. Khan, W. Ahmad, A.A.M. Amin, A. Nafees, New shapley additive ExPlanations (SHAP) approach to evaluate the raw materials interactions of steel-fiber-reinforced concrete, Materials 15 (2022) 6261, http://dx.doi.org/10.3390/ma15186261.
[128] M. Vahab, E. Haghighat, M. Khaleghi, N. Khalili, A physics-informed neural network approach to solution and identification of biharmonic equations of elasticity, J. Eng. Mech. 148 (2022) 1–21, http://dx.doi.org/10.1061/(asce)em.1943-7889.0002062.
[129] S. Rojas, P. Maczuga, J. Muñoz-Matute, D. Pardo, M. Paszynski, Robust variational physics-informed neural networks, Comput. Methods Appl. Mech. Engrg. (2023) 1–21, http://dx.doi.org/10.1016/j.cma.2024.116904.
[130] S. Cuomo, V.S. Di Cola, F. Giampaolo, G. Rozza, M. Raissi, F. Piccialli, Scientific machine learning through physics–informed neural networks: Where we are and what's next, J. Sci. Comput. 92 (3) (2022) 88, http://dx.doi.org/10.1007/s10915-022-01939-z.
[131] R. Pu, X. Feng, Physics-informed neural networks for solving coupled Stokes–Darcy equation, Entropy 24 (2022) http://dx.doi.org/10.3390/e24081106.
[132] C. Xiao, X. Zhu, F. Yin, X. Cao, Physics-informed neural network for solving coupled Korteweg-de Vries equations, JPCS (2021) http://dx.doi.org/10.1088/1742-6596/2031/1/012056.
[133] J. Yu, L. Lu, X. Meng, G. Karniadakis, Gradient-enhanced physics-informed neural networks for forward and inverse PDE problems, Comput. Methods Appl. Mech. Engrg. 393 (2022) http://dx.doi.org/10.1016/j.cma.2022.114823.
[134] C. Chen, G. Gu, Physics-informed deep-learning for elasticity: Forward, inverse, and mixed problems, Adv. Sci. 10 (2023) 1–11, http://dx.doi.org/10.1002/advs.202300439.
[135] S. Thakur, M. Raissi, A. Ardekani, ViscoelasticNet: A physics informed neural network framework for stress discovery and model selection, 2022, pp. 1–21, http://dx.doi.org/10.48550/arXiv.2209.06972, arXiv:2209.06972.
[136] J. Lee, Anti-derivatives approximator for enhancing physics-informed neural networks, Comput. Methods Appl. Mech. Engrg. 426 (2024) 117000, http://dx.doi.org/10.1016/j.cma.2024.117000.
[137] Z. Li, J. Yoon, R. Zhang, F. Rajabipour, W.V. Srubar III, I. Dabo, A. Radlińska, Machine learning in concrete science: applications, challenges, and best practices, NPJ Comput. Mater. 8 (1) (2022) 127, http://dx.doi.org/10.1038/s41524-022-00810-x.